MECHANICAL AND THERMAL BUCKLING

OF THIN FILMS

A Thesis presented to the Faculty of the Graduate School

University of Missouri-Columbia

In Partial Fulfillment

Of the Requirements for the Degree

Master of Science

---

by

SUMA PASPULETI

Dr. Frank Z. Feng, Thesis Supervisor

JULY 2005

The undersigned, appointed by the Dean of the Graduate School,

have examined the thesis entitled.

MECHANICAL AND THERMAL BUCKLING OF THIN FILMS

Presented by Suma Paspuleti

A candidate for the degree of Master of Science

And hereby certify that in their opinion it is worthy of acceptance.

Frank Z. Feng, Professor, Dept. of Mechanical and Aerospace Engineering

Frank P. Pai, C. W. LaPierre Professor, Dept. of Mechanical and Aerospace Engineering

Tushar K. Ghosh, Professor, Dept. of Nuclear Engineering

ACKNOWLEDGEMENTS

My sincere thanks to the University of Missouri-Columbia in general, and the Mechanical and Aerospace Engineering department in specific, for providing me the opportunity for a Masters program. I am grateful to Dr. Frank Feng for not only serving as the Chairperson of my Masters Advisory Committee, but also for the support extended without which this thesis would not have been possible. I would also like to thank Dr. Frank Pai and Dr. Tushar Ghosh for being members on my committee and for their valuable guidance.

My gratitude to my colleagues who have given me helpful suggestions and to my friends who have helped me accomplish my thesis. Finally, I thank my parents and my family for their constant encouragement and support.

TABLE OF CONTENTS

LIST OF FIGURES

Figure

LIST OF TABLES

Table

MECHANICAL AND THERMAL BUCKLING OF THIN FILMS

Suma Paspuleti

Dr. Frank Z. Feng, Thesis Supervisor
Department of Mechanical & Aerospace Engineering

ABSTRACT

Devices with feature size on the order of one micrometer have found widespread applications in science and engineering. MEMS, is a rapidly growing technology for the fabrication of miniature devices which provides a way to integrate mechanical, fluidic, optical, and electronic functionality on very small devices, ranging from 0.1 microns to one millimeter. Recently, it has been proposed that regular patterns can be generated through the mechanical buckling of a thin film. In this thesis, we focus on the buckling mechanism. The wavy patterns are generated when the thin elastic film is subjected to an in-plane compressive stress and by the application of controlled heating. We first introduce the mechanism of developing wave patterns through buckling using beam buckling as an example and then the finite element formulation and the commercial analysis package Algor. Our study includes the “stress stiffening” component, which is not usually included in most finite element analyses. Both the ‘Critical Buckling Load and the ‘Natural Frequency with Load Stiffening’ analyses are made use of to determine the buckling loads. Finally, the buckling load for each case is determined through the analysis and a comparison with the theoretical values is made.

Chapter 1

INTRODUCTION

1.1 Historical Background of MEMS

The field of microelectronics began in 1948 when the first transistor was invented, which then became obsolete in the 1950s following the development of the bipolar junction transistor and then the junction field-effect transistor [1]. These two types of electronic devices are at the heart of all microelectronic components, but it was the development of integrated circuits (ICs) in 1958 that spawned today's computer industry. IC technology has developed rapidly during the past 40 years but their complexity doubled every 2-3 years since 1970 [2].

Devices with feature size on the order of one micrometer have found widespread applications in science and engineering. Micro-Electro-Mechanical Systems, or MEMS, is a rapidly growing technology for the fabrication of miniature devices using processes similar to those used in the integrated circuit industry. The use of these miniaturization technologies confers advantages beyond the obvious decreases in physical volume and weight, such as increased performance and reliability, and decreased cost. In the most general sense, MEMS attempts to exploit and extend the fabrication techniques developed for the IC industry to add mechanical elements, such as beams, gears,

diaphragms, and springs, to the electrical circuits to make integrated microsystems for perception and control of the physical world [1, 2].

MEMS devices are actually the interface between the physical world and the electronic world. On one hand, this reality greatly complicates the design, production, implementation, and performance qualifications for any single application. On the other hand, a vastly broader and more diverse range of utility for MEMS devices, from optical fiber switching, to fluid control, to micromechanical electrical relays, to biosensors is made possible. MEMS technology provides a way to integrate mechanical, fluidic, optical, and electronic functionality on very small devices, ranging from 0.1 microns to one millimeter. Combining these functions onto a single device provides capabilities that other fabrication technologies simply could not deliver. Examples are miniature sensors and actuators for monitoring and control of physical systems. Increasingly, these devices are finding applications in the life science research. With platform materials such as glass, polymers, silicon or nanostructures combined with biomaterials like DNA, proteins, in vivo, in vitro or cells, applications such as biosensing, tissue engineering, drug delivery, blood analysis, point of care and biocomputing can be achieved [3, 4, 5, 6].

1.2 Overview of the Fabrication Process

The three characteristic features of MEMS fabrication technologies are miniaturization, multiplicity, and microelectronics. Miniaturization is clearly an important part of MEMS, since materials and components that are relatively small and light enable compact and quick-response devices. Multiplicity refers to the batch

fabrication inherent in semiconductor processing. Finally, microelectronics provides the intelligence to MEMS and allows the monolithic merger of sensors, actuators, and logic to build closed-loop feedback components and systems. Clearly, the successful miniaturization and multiplicity of traditional electronics systems would not have been possible without IC fabrication technology. It is therefore natural that the IC fabrication technology, or microfabrication, has so far been the primary enabling technology for the development of MEMS [2].

Microfabrication is traditionally accomplished through lithography and etching of silicon. Microsystems almost always involve complex three-dimensional structural geometry in microscale, and patterning of geometry with extremely high precision at this scale is a major challenge to engineers. *Photolithography* or *microlithography* is the only viable way for producing high-precision patterning on substrates in microscale at the present time.

The photolithography process involves the use of an optical image and a photosensitive film to produce a pattern on a substrate and is one of the most important steps in microfabrication. The process begins with the substrate, which can be a silicon wafer or other material such as silicon dioxide or silicon nitride. In this process, a photoresist is first coated onto the flat surface of the substrate and the substrate with photoresist is then exposed to a set of lights through a transparent mask with the desired patterns. Photoresist materials change their solubility when they are exposed to light. Photoresists that become more soluble under light are classified as *positive photoresists*, whereas the ones that are more soluble under the shadow are termed as *negative photoresists*. The exposed substrate after development with solvents will have opposite

effects in these two types of photoresists. The retained photoresist materials create the imprinted patterns after the development. The pattern of the substrate under the shadow of the photoresist is protected from the subsequent etching. A permanent pattern is thus created in the substrate after the removal of the photoresist [7]. A schematic diagram of the procedure is shown in *Figure 1.1*.

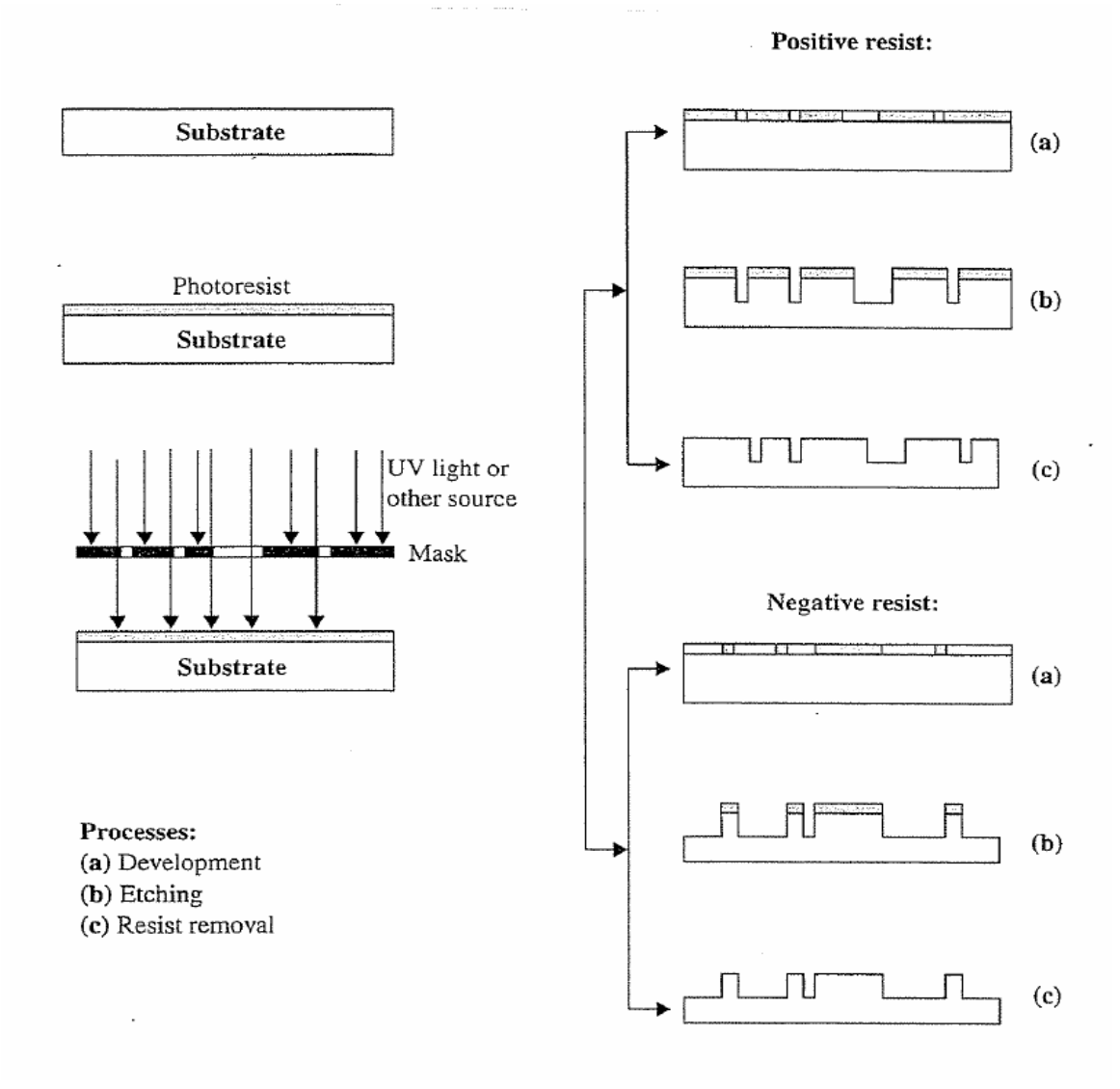

Figure 1.1 Photolithography process [7]

1.3 Pattern Generation by Buckling of Thin Films: A Recently Proposed study

Recently, it has been proposed that regular patterns can be generated through the mechanical buckling of a thin film [8, 9]. Here, a planar surface of poly (dimethylsiloxane) PDMS, previously soaked in a solution of benzophenone in dichloromethane, is exposed to UV irradiation through an amplitude photomask. The exposed regions become stiffer and less elastomeric. Now, the sample – with its surface patterned into regions differing in stiffness and coefficient of thermal expansion, is heated and it expands. A thin metal film of Ti and Au is deposited onto the surface by e-beam evaporation. The sample is then cooled; this cooling places the gold film under compressive stress. To relieve these stresses, the thin metal film buckles. The photostiffened regions provide more resistance to buckling than those not stiffened; this difference in response creates a pattern of buckles and this pattern of buckles is thus related to the pattern of the mask used in the UV irradiation step. The schematic diagram of the procedure is shown in *Figure 1.2*.

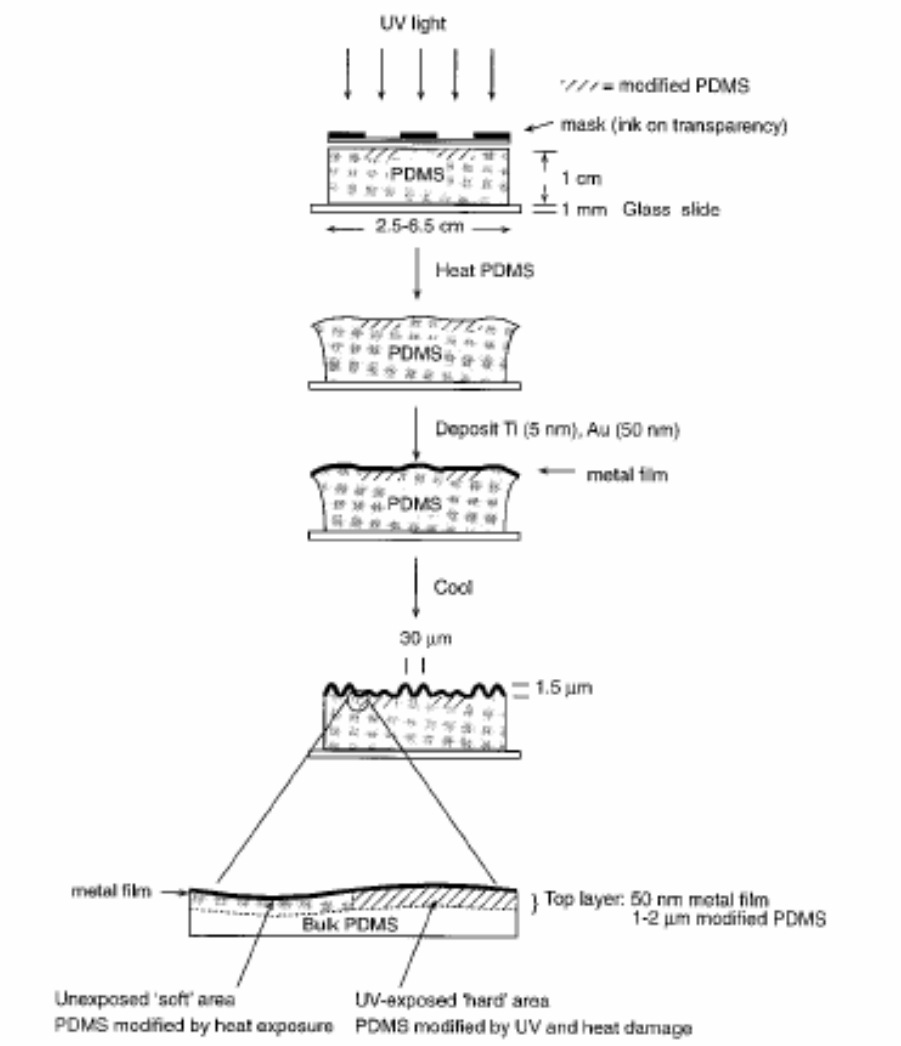

Figure 1.2 Outline of the procedure used to obtain aligned buckles on patterned PDMS [8]

1.4 Thesis Outline

In this thesis, we apply the finite element methods to study the buckling of thin structures under compressive load which can be generated through selective heating.

In chapter 2, we first explore the capabilities of the Algor program in conducting the buckling analysis. The numerical results are compared with the analysis for simple geometries to examine the accuracy of the Algor software.

In chapter 3, we study the buckling of the beam under compressive axial loads as well as under thermal loads.

In the same fashion, in chapter 4, we study the buckling mechanisms of plates. The additional aspect in this chapter is the introduction of localized force and thermal loads.

Chapter 5 is an attempt to validate the results obtained in the previous ones, namely, chapters 3 and 4. This is accomplished by the calculation of natural frequencies of the beams and plates using the Algor finite element package.

Chapter 2

FINITE ELEMENT FORMULATION WITH STRESS STIFFENING

Regular wavy patterns on a thin elastic film can be generated in various ways. In this thesis, we focus on the buckling mechanism. The wavy patterns are generated when the thin elastic film is subjected to an in-plane compressive stress. The in-plane compressive stress is more easily generated by the application of controlled heating. With constraints, compressive thermal stresses develop in the film. In microfabrication, heating can be achieved through light radiation. To achieve desired patterns at selected areas, masks can be used to direct the radiation. This process is very compatible with the lithography process.

In this chapter, we first introduce the mechanism of developing wave patterns through buckling using beam buckling as an example. We then introduce the finite element formulation and the commercial analysis package, Algor that will be used in the subsequent analysis. The finite element formulation includes the “stress stiffening” component, which is not usually included in many finite element analyses.

2.1 Critical Load of a Simply-supported Beam under Compressive Loads

Consider a simply supported beam shown in *Figure 2.1*. If the column is fully aligned, the applied compressive load *P* can be increased until one reaches the compressive strength of the material. Yet, in reality the column will fail due to buckling as shown in the figure on the right in *Figure 2.1* long before this load is reached [10]. Buckling can be catastrophic if it occurs in the normal use of most products. Once the geometry starts to deform, it can no longer withstand even a fraction of the initially applied force [11].

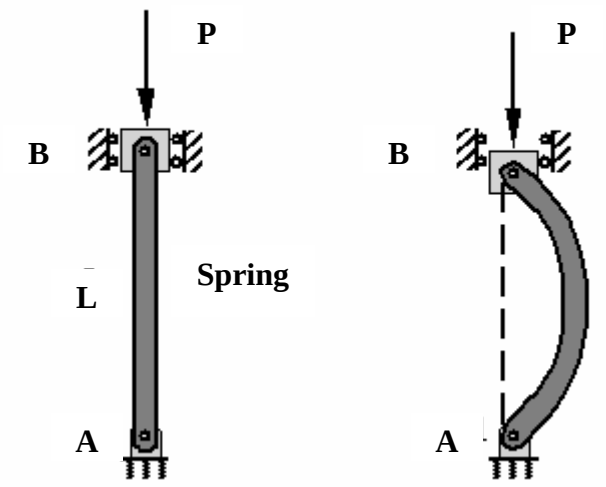

Figure 2.1 A Simply-supported beam

The equation governing the deflection is given as:

$$\frac{d^2w}{dx^2} + \frac{P}{EI}w = 0 \tag{2.1}$$

where

$w =$ Displacement of the beam;

P = Applied compressive load;

E = Young's Modulus of the material of the beam (Steel); and

I = Moment of inertia of the beam.

This is a second order homogeneous ordinary differential equation with constant coefficients that has a solution of the form

$$w = C_1 \sin(\lambda x) + C_2 \cos(\lambda x) \tag{2.2}$$

For the beam to have a nontrivial solution (buckled solution), one must select $\lambda = \frac{n\pi}{l}$.

To get a nontrivial solution to the buckling problem, the axial load must satisfy the relation $P = EI\lambda^2$, which results in the expression for the critical load given by

$$P_{cr} = \frac{n^2\pi^2 EI}{L^2} \tag{2.3}$$

Obviously, the smallest critical load is associated with *n*=1. Therefore, the column will buckle at the load associated with the first buckling mode if the column is not restricted from taking the shape associated with this mode [10].

Therefore, we finally get the critical load as:

$$P_{cr} = \frac{\pi^2 EI}{L^2} \tag{2.4}$$

and the corresponding mode shape is shown in *Figure 2.2*.

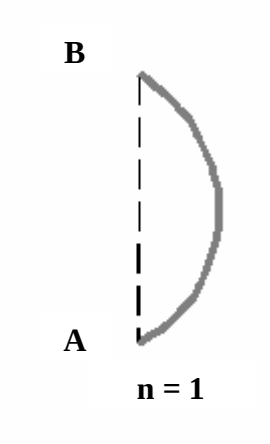

Figure 2.2 The first mode shape of a Simply-supported beam

Now, consider a cantilever beam as shown in *Figure 2*.3. The result (2.4) may be applied to that of a cantilever beam. A cantilever beam may be regarded as one half of a simply-supported beam. Its critical load can be obtained from the formula (2.4) by replacing L by $2L$ to get:

$$P_{cr} = \frac{\pi^2 EI}{4L^2} \tag{2.5}$$

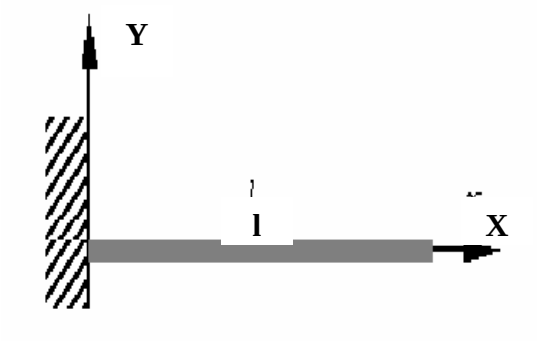

Figure 2.3 A Cantilever beam

2.2 Buckling Analysis using Finite Element Method

2.2.1 Introduction to Finite Element Analysis

The term “finite element” was first used by Clough in 1960 [12]. Since its inception, the literature on finite element applications has grown exponentially, and today there are numerous journals that are primarily devoted to the theory and application of the method.

The most distinctive feature of the finite element method that separates it from others is the division of a given domain into a set of simple subdomains, called *finite elements*. Any geometric shape that allows computation of the solution or its approximation, or provides necessary relations among the values of the solution at selected points, called *nodes*, of the subdomain, qualifies as a finite element. Other features of the method include seeking continuous, often polynomial, approximations of the solution over each element in terms of nodal values, and assembly of element equations by imposing the interelement continuity of the solution and balance of interelement forces [12].

2.2.2 Derivation of the Mass and Stiffness Matrices

Let us consider the beam element shown in *Figure 2.4.*

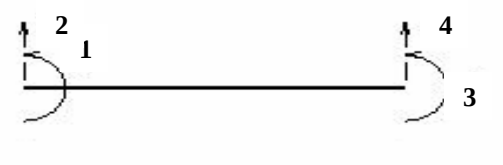

Figure 2.4 Beam element

The transverse deflection *w* of the beam is governed by the fourth-order differential equation

$$\frac{d^2}{dx^2}\left(EI\frac{d^2w}{dx^2}\right) = f(x) \text{ for } 0 < x < l \tag{2.6}$$

where 'l' is the length of the beam element.

As shown in the *Figure 2.4*, let 2 and 4 represent the displacements at the two nodes, namely $u_1(t)$ and $u_3(t)$ respectively and let 1 and 3 represent the slopes at the two nodes, namely $u_2(t)$ and $u_4(t)$ respectively. It follows from equation (2.6) that the transverse static displacement must satisfy the following condition:

$$\frac{d^2}{dx^2}\left[EI\frac{d^2u(x,t)}{dx^2}\right] = 0 \tag{2.7}$$

On integrating equation (2.7), we get:

$$u(x,t) = C_1(t)x^3 + C_2(t)x^2 + C_3(t)x + C_4(t) \tag{2.8}$$

The boundary conditions can be obtained from the *Figure 2.4* as follows:

$$u(0,t) = u_1(t) \quad u_x(0,t) = u_2(t)$$

$$u(l,t) = u_3(t) \qquad u_x(l,t) = u_4(t) \tag{2.9}$$

On applying these boundary conditions to equation (2.8), we get:

$$C_1(t) = \frac{1}{l^3}\left[2(u_1(t) - u_3(t)) + l(u_2(t) + u_4(t))\right] \tag{2.10}$$

$$C_2(t)=\frac{1}{l^2}\left[3(u_3(t)-u_1(t))-l(2u_2(t)+u_4(t))\right] \tag{2.11}$$

$$C_3(t)=u_2(t) \tag{2.12}$$

$$C_4(t)=u_1(t) \tag{2.13}$$

Substituting the equations (2.10)-(2.13) in the equation (2.8) and rearranging the terms, the approximate displacement $u(x,t)$ can be expressed as:

$$u(x,t)=\left(1-\frac{3x^2}{l^2}+\frac{2x^3}{l^3}\right)u_1(t)+l\left(\frac{x}{l}-\frac{2x^2}{l^2}+\frac{x^3}{l^3}\right)u_2(t)+\left(\frac{3x^2}{l^2}-\frac{2x^3}{l^3}\right)u_3(t)+l\left(-\frac{x^2}{l^2}+\frac{x^3}{l^3}\right)u_4(t)$$

$$=\left\{1-\frac{3x^2}{l^2}+\frac{2x^3}{l^3},x-\frac{2x^2}{l}+\frac{x^3}{l^2},\frac{3x^2}{l^2}-\frac{2x^3}{l^3},-\frac{x^2}{l}+\frac{x^3}{l^2}\right\}\begin{Bmatrix}u_1(t)\\u_2(t)\\u_3(t)\\u_4(t)\end{Bmatrix} \tag{2.14}$$

In the finite element method, the assumed displacement shape functions relate the generic displacements to nodal displacement as follows:

$$u(x,t)=\{N\}^T\{q(t)\} \tag{2.15}$$

Hence, from equation (2.14), the linear displacement shape function vector is given by

$$\{N\}=\left\{1-\frac{3x^2}{l^2}+\frac{2x^3}{l^3},x-\frac{2x^2}{l}+\frac{x^3}{l^2},\frac{3x^2}{l^2}-\frac{2x^3}{l^3},-\frac{x^2}{l}+\frac{x^3}{l^2}\right\}^T \tag{2.16}$$

and the nodal displacement vector is given by

$$\{q(t)\}=\begin{Bmatrix}u_1(t)\\u_2(t)\\u_3(t)\\u_4(t)\end{Bmatrix} \tag{2.17}$$

Therefore, the mass matrix, M can be represented as follows:

$$M=\int\rho\{N\}\{N\}^T\,dv=\int_0^l\rho A\{N\}\{N\}^T$$

$$= \rho A \int_0^l \begin{Bmatrix} 1-\frac{3x^2}{l^2}+\frac{2x^3}{l^3} \\ x-\frac{2x^2}{l}+\frac{x^3}{l^2} \\ \frac{3x^2}{l^2}-\frac{2x^3}{l^3} \\ -\frac{x^2}{l}+\frac{x^3}{l^2} \end{Bmatrix} \left\{1-\frac{3x^2}{l^2}+\frac{2x^3}{l^3}, x-\frac{2x^2}{l}+\frac{x^3}{l^2}, \frac{3x^2}{l^2}-\frac{2x^3}{l^3}, -\frac{x^2}{l}+\frac{x^3}{l^2}\right\} dx \tag{2.18}$$

On evaluating the above integrals, we get:

$$M = \frac{\rho A l}{420} \begin{bmatrix} 156 & 22l & 54 & -13l \\ 22l & 4l^2 & 13l & -3l^2 \\ 54 & 13l & 156 & -22l \\ -13l & -3l^2 & -22l & 4l^2 \end{bmatrix} \tag{2.19}$$

Also, the stiffness matrix is given by:

$$K = \int B^T E B dv$$

where the strain displacement matrix, $B = d\{N\}^T$ and the linear differential operator d can be given by:

$$d = -y\frac{d^2}{dx^2}$$

Therefore, B can be written as:

$$B = -y\frac{d^2\{N\}^T}{dx^2} = -\frac{y}{l^3}\left\{12x-6l, 6lx-4l^2, -12x+6l, 6lx-2l^2\right\}.$$

Now,

$$K = \int_0^l \int_A \frac{Ey^2}{l^6} \begin{Bmatrix} 12x-6l \\ 6lx-4l^2 \\ -12x+6l \\ 6lx-2l^2 \end{Bmatrix} \left\{12x-6l, 6lx-4l^2, -12x+6l, 6lx-2l^2\right\} dA dx$$

$$= \frac{E}{l^6}\int_0^l \begin{Bmatrix} 12x-6l \\ 6lx-4l^2 \\ -12x+6l \\ 6lx-2l^2 \end{Bmatrix} \{12x-6l, 6lx-4l^2, -12x+6l, 6lx-2l^2\} dx \int_A y^2 dA \qquad (2.20)$$

On evaluating the above integrals, we get:

$$K = \frac{EI}{l^3}\begin{bmatrix} 12 & 6l & -12 & 6l \\ 6l & 4l^2 & -6l & 2l^2 \\ -12 & -6l & 12 & -6l \\ 6l & 2l^2 & -6l & 4l^2 \end{bmatrix} \qquad (2.21)$$

where

'E' is the Young's modulus and 'I' is the moment of inertia [13, 14].

2.2.3 Derivation of the Stress Stiffness Matrix

2.2.3.1 Stress Stiffening and Buckling

The term stress stiffening refers to the influence of membrane forces on lateral deflection, especially the lateral deflection associated with bending of beams, plates and shells. Membrane forces, and associated membrane stresses, act along the axis of a bar or a beam and tangent to the midsurface of a plate or a shell. Despite the name "stress stiffening", resistance to bending deformation is reduced when membrane forces are compressive rather than tensile, as when a column carries a compressive axial load.

Buckling means loss of the stability of an equilibrium configuration, without fracture or separation of the material or at least prior to it. Bifurcation buckling is the

kind of buckling in which, for an axial compressive load of magnitude P_{cr}, called the critical load, the straight pre-buckling configuration ceases to be a stable state of equilibrium and an alternative buckled configuration is also possible at load P_{cr}. Buckling may also appear without bifurcation, as at a limit point, where there is no alternative and infinitesimally close equilibrium configuration.

In finite element analysis, the effects of membrane stresses on lateral deflection are accounted for by a matrix $[k_\sigma]$, which augments the conventional stiffness matrix $[k]$. Matrix $[k_\sigma]$ is a function of an element's geometry, displacement field, and state of membrane stress, and is called the stress stiffness matrix. It is also called as "initial stress stiffness matrix" and "geometric stiffness matrix".

Matrix $[k_\sigma]$ is independent of material properties and is therefore applicable despite possible anisotropy and yielding. Element $[k_\sigma]$ matrices are assembled to provide structural matrix $[K_\sigma]$ in the same way that conventional element stiffness matrices [K] are assembled to provide [K] [15].

2.2.3.2 Analysis of a Beam-Column

Let us consider a simply-supported beam. An axial force *P*, positive in tension, is regarded imposed at the outset, perhaps by a change in temperature while the ends of the bar are not allowed to move axially. An analysis based on energy concepts is as follows:
For small lateral displacement $v = v(x)$, strain energy in bending is given by the expression in terms of curvature $v_{,xx}$.

$$U_b = \frac{1}{2}\int_0^L EI_z v^2{}_{,xx}\,dx \tag{2.22}$$

Imagine that $v = v(x)$ takes place without any axial displacement *u*. Each differential length *dx* becomes a new differential length *ds*, where *ds*>*dx*. The expression for *ds* is given as:

$$ds = \sqrt{1 + v^2{}_{,x}}\,dx$$

$$ds \approx \left(1 + \frac{1}{2}v^2{}_{,x}\right)dx \tag{2.23}$$

Axial membrane strain in the bar is therefore

$$\varepsilon_m = \frac{ds - dx}{dx} = \frac{ds}{dx} - 1$$

Hence, $\varepsilon_m = \left(1 + \frac{1}{2}v^2{}_{,x}\right) - 1 = \frac{1}{2}v^2{}_{,x}$ (2.24)

During small lateral displacement, axial force *P* remains essentially constant. As each elemental length *dx* lengthens an amount $\varepsilon_m dx$, the tensile force *P* it carries, does work, and stores strain energy, in the amount $P\varepsilon_m dx$. Thus, the change in membrane energy is

$$U_m = \int_0^L P\varepsilon_m dx \quad \text{or} \quad U_m = \frac{1}{2}\int_0^L Pv^2{}_{,x}\,dx \tag{2.25}$$

Now, let a straight bar or a beam lie along the x axis, and let lateral displacement *v* and rotation $v_{,x}$ in the xy plane be determined by nodal d.o.f. $\{d\}$. Thus

$$v = [N]\{d\} \text{ and } v_{,x} = [G]\{d\} \text{ where } [G] = \frac{d}{dx}[N] \tag{2.26}$$

Membrane strain energy U_m associated with lateral displacement *v* is given by equation (2.25). With axial force *P* considered positive in tension,

$$U_m = \frac{1}{2}\int_0^L Pv^2{}_{,x}\,dx = \frac{1}{2}\int_0^L v_{,x}{}^T Pv_{,x}\,dx = \frac{1}{2}\{d\}^T[k_\sigma]\{d\} \tag{2.27}$$

where stress stiffness matrix $[k_\sigma]$ is given by

$$[k_\sigma] = \int_0^L [G]^T[G]P\,dx \tag{2.28}$$

If lateral displacement is also allowed in the z direction, additional d.o.f.s are needed in $\{d\}$ and displacement *w* is included in calculations. The resulting $[k_\sigma]$ matrices are very similar to those for plane deformation but contain more terms [15].

2.3 Buckling Analysis using Algor

2.3.1 Type of Analysis

The 'Critical buckling load analysis' (also known as 'Eigenvalue buckling analysis') is employed here. It examines the geometric stability of models under primarily axial load. Buckling analysis is used to determine if a specified set of loads will cause buckling and to find the shape of the buckling mode. It is useful in situations where a part or assembly is subjected to an axial load or when a model undergoes edge compression. Engineers can then design supports or stiffeners to prevent local buckling.

Buckling analyses are routinely conducted in the following applications:

- Automotive frame design
- Column design
- Infrastructure design

- Safety factor determination
- Slender member design
- Structural integrity verification
- Transmission tower design
- Uniform Building Code (UBC) validation
- Vehicle skin design [11].

2.3.2 Geometry and Material Properties of a Test Case

We consider a cantilever beam with geometry given in *Figure 2.5*. The beam has a length of 8 in, breadth of 0.2 in and a thickness of 0.1 in.

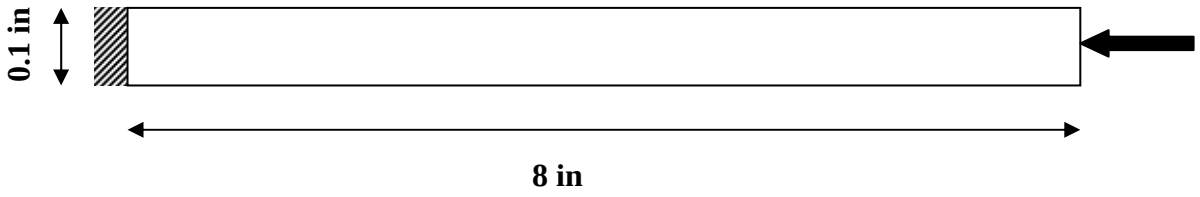

Figure 2.5 Beam geometry

The beam is assumed to be made of steel. The relevant material properties are given in *Table 2.1* [16].

Table 2.1 Material properties of Steel

Mass density	7.35×10^{-4} Lb-f-s^2 / in^4
Modulus of Elasticity	29×10^6 Lb-f / in^2
Poisson's Ratio	0.29
Thermal Coefficient of Expansion	6.5×10^{-6} / ^oF
Shear Modulus of Elasticity	11.2×10^6 Lb-f / in^2

2.3.3 Analysis of a Beam under an Axial Load

2.3.3.1 Analysis Procedures

1. Go to the 'Start menu' and pull up 'Programs', 'Algor', 'Superdraw III'.
2. Go to 'Add', 'Line' and add a line 8 inches long.
3. Go to 'Construct', 'Divide' and set the number to, say, 10 and hit the divide button. This will break down your beam into 10 elements.
4. Transfer the model to the FEA Editor by going to 'File', 'Export to Fempro'.
5. A 'Units definition' screen appears. Click 'OK' to set it to the default units.
6. Set the 'Analysis type' to 'Critical Buckling Load Analysis'.
7. Set the 'Element type' to 'Beam'.
8. Double click on the 'Element definition', highlight any field, say the 'Area', click on 'Cross-section libraries' and in the top right corner of the dialog box select

'Rectangular'.

9. Enter the dimensions (b=0.2" and h=0.1").
10. Click 'OK' twice.
11. Set the 'Material' to 'Steel (ASTM-A36)'.
12. Select one of the endpoints of the beam using 'Vertices-select' or 'Rectangular-select', and constrain all the degrees of freedom of this end.
13. Select the other end of the beam and assign the required value of an axial force in the negative x-direction.
14. Now, after setting up the model, along with the required boundary conditions and loads, click on the 'Check model' icon at the top toolbars; this is to run a check to see if everything was done right or not.
15. After checking the model, run the analysis.
16. After the analysis is done, the results of the analysis are displayed in 'Superview'.
17. Go to the 'Analysis summary' in order to obtain the 'Buckling Load Multiplier'.

2.3.3.2 Analysis Results and Discussion

For the cantilever beam with an axial load at the free end, the critical load is calculated according to equation (2.5).

$$P_{cr} = \frac{\pi^2 EI}{4L^2}$$

For the geometry and material of the test case, we find the critical load to be as

$$P_{cr} = 18.7248 \ \ lbf \tag{2.29}$$

For the different axial loads applied, the corresponding buckling load multipliers are given in *Table 2.2*. The total buckling load is the product of the applied load and its corresponding buckling load multiplier. Here, the load is applied at the free end of the beam in the negative x-direction.

Table 2.2 Results for different axial loads

Load (Lb-f)	Buckling Load Multiplier
1	18.6359
5	3.72719
10	1.86359

Hence, the buckling load from *Table 2.2* is: 1 x 18.6359 = 18.6359 Lb-f, which is almost the same as the one obtained through hand calculations.

Algor also gives the eigenvector corresponding to the eigenvalue at the buckling load. The eigenvector is the buckling mode. For the cantilever beam studied above, the buckling mode is shown in *Figure 2.6*.

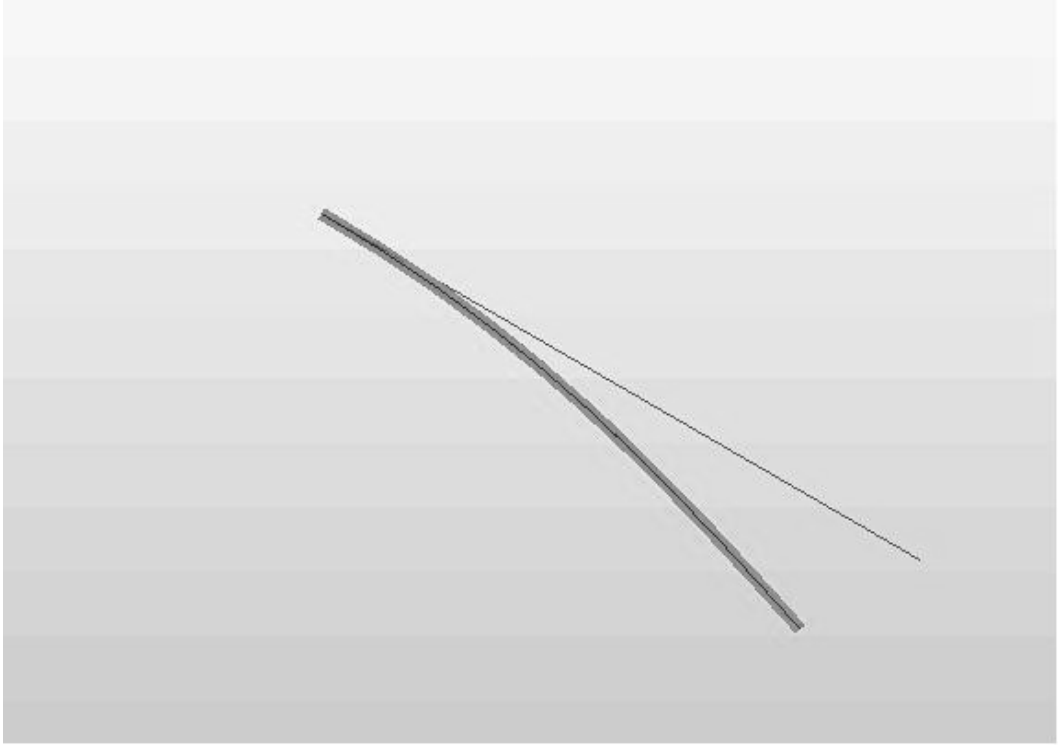

Figure 2.6 Buckling mode

Chapter 3

BUCKLING ANALYSIS OF A BEAM

Since this work is motivated by generating wavy patterns, we are interested to know if it is possible to cause higher modes to buckle at a lower buckling load for a carefully applied load.

In this section, two types of loads are considered. In the first case, the beam is subjected to an axial load. In the second case, the beam is subjected to a thermal load.

3.1 Buckling under Axial Loads

We consider a clamped-clamped beam with the same geometry and material properties as given in section 2.3.2 of chapter 2.

The beam is subjected to an axial load as shown in *Figure 3.1*. We examine the variation in buckling loads as the axial position of the load application, shown as 'x' in *Figure 3.1*, changes.

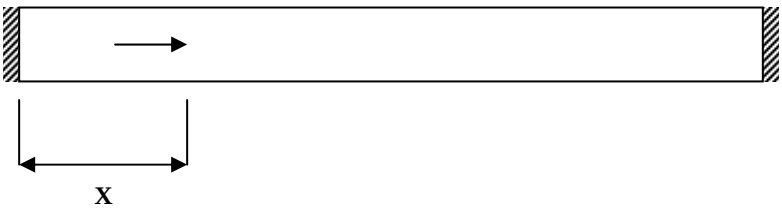

Figure 3.1 Beam geometry

3.1.1 Analysis Procedures

1. Go to the ‘Start menu’ and pull up ‘Programs’, ‘Algor’, ‘Superdraw III’.
2. Go to ‘Add’, ‘Line’ and add a line 8 inches long.
3. Go to ‘Construct’, ‘Divide’ and set the number to

   (i) 20 in the first case where the beam would be divided into 20 elements; and

   (ii) 40 in the second case where the beam would be divided into 40 elements

   Now hit the divide button. This will break down your beam into the required number of elements.
4. Transfer the model to the FEA Editor by going to ‘File’, ‘Export to Fempro’.
5. A Units Definition screen appears. Click ‘OK’ to set it to the default units.
6. Set the ‘Analysis type’ to ‘Critical Buckling Load Analysis’.
7. Set the ‘Element type’ to ‘Beam’.
8. Double click on the ‘Element definition’, highlight any field, say the ‘Area’, and click on ‘Cross-section libraries’ and in the top right corner of the dialog box select ‘Rectangular’.
9. Enter the dimensions (b=0.2” and h=0.1”).
10. Click ‘OK’ twice.
11. Set the ‘Material’ to ‘Steel (ASTM-A36)’.
12. Select both the endpoints of the beam using ‘Vertices-select’ or ‘Rectangular- select’, and constrain all the degrees of freedom of this end.
13. Start with the left-most node of the beam and apply the required value of axial force in the positive x-direction, as shown in *Figure 3.2* and *Figure 3.3*. (For each analysis,

apply a pointed axial load at every node or every alternate load as per the requirement and proceed towards the right-most end of the beam).

Figure 3.2 Axial load applied at the 3rd node of the beam element

Figure 3.3 Axial load applied at the 11th node of the beam element

14. Now, after setting up the model, along with the required boundary conditions and loads, click on the ‘Check Model’ icon at the top toolbars; this is to run a check to see

if everything was done right or not.

15. After checking the model, run the analysis.

16. After the analysis is done, the results of the analysis are displayed in Superview.

17. Go to the ‘Analysis summary’ in order to obtain the ‘Buckling Load Multiplier’.

3.1.2 Analysis Results

Table 3.1 gives the buckling loads corresponding to different axial positions of the load.

Table 3.1 Results for axial loads - 20 elements

Node#	X (in)	Load Value (Lb-f)	Buckling Load Multiplier Value (=Critical Buckling Load)
1	0	1	Error
2	0.05	1	6182.65
3	0.1	1	4010.89
4	0.15	1	-2018.14
5	0.2	1	-1503.70
6	0.25	1	-1309.54
7	0.3	1	-1285.54
8	0.35	1	-1405.26
9	0.4	1	1629.57
10	0.45	1	1691.80
11	0.5	1	2905.13

12	0.55	1	-1686.32
13	0.6	1	-5537.92
14	0.65	1	1405.84
15	0.7	1	1285.54
16	0.75	1	1309.54
17	0.8	1	1503.70
18	0.85	1	2018.15
19	0.9	1	7908.21
20	0.95	1	-6182.65
21	1.0	1	Error

Table 3.2 Results for axial loads - 40 elements

Node #	X (in)	Load Value (Lb-f)	Buckling Load Multiplier Value (= Critical Buckling Load)
1	0	1	Error
3	0.05	1	6180.42
4	0.075	1	4289.24
5	0.1	1	12833.8
6	0.125	1	-2542.51
14	0.325	1	-1326.16
15	0.35	1	-1404.78
16	0.375	1	-1620.73
17	0.4	1	2066.54
18	0.425	1	1654.69

19	0.45	1	1935.52
20	0.475	1	1875.68
21	0.5	1	-3666.50
22	0.525	1	-1741.18
23	0.55	1	-1847.32
24	0.575	1	-1650.80
25	0.6	1	-1631.21
26	0.625	1	20493.4
27	0.65	1	1449.10
36	0.875	1	2545.78
37	0.9	1	12502.0
41	1.0	1	Error

A graph is plotted between the position of the axial load on the X-axis and the critical buckling load on the Y-axis for the 20-element beam as well as the 40-element beam and both the graphs are overlapped as shown in *Figure 3*.4 so that a comparison can be made.

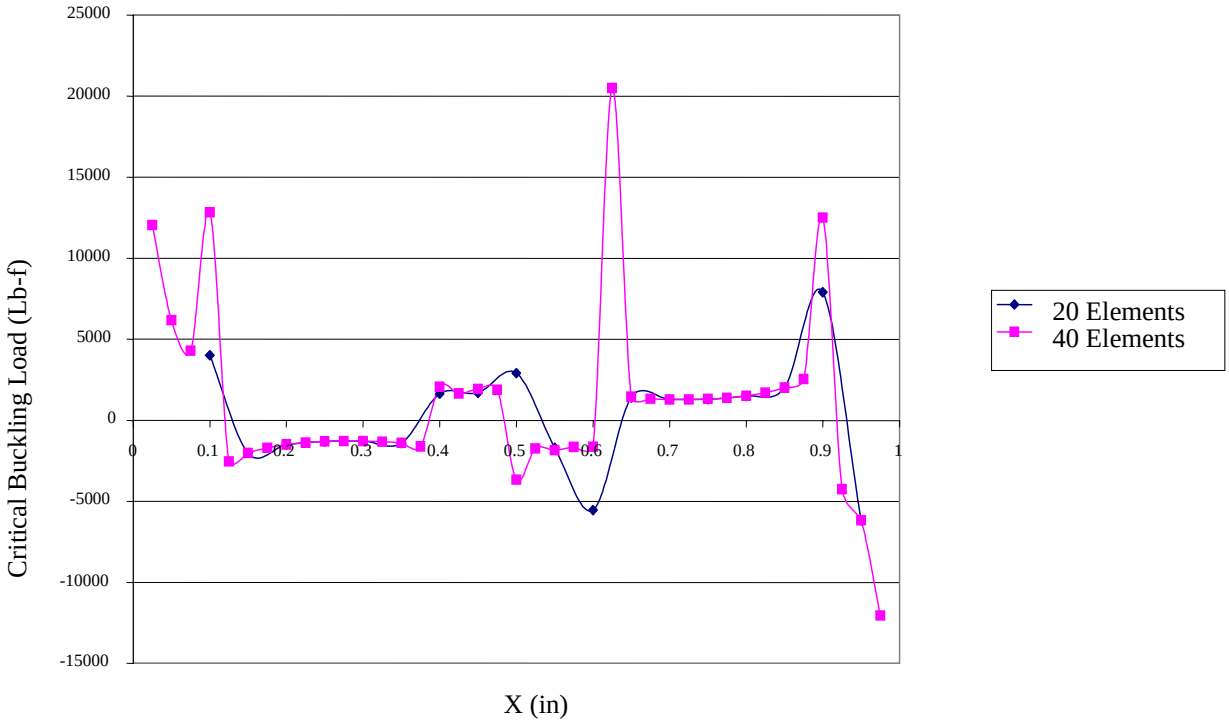

Figure 3.4 Graph depicting the variation of the critical buckling loads with respect to x for the 20-element and the 40-element beams

3.1.3 Results with increased Number of Iterations and Discussion

In the previous section, i.e. section 3.1.2, we see that some of the buckling loads did not match properly for the 20-element beam and the 40-element beam. We introduce this section, here, as an improvement in the method for obtaining the buckling loads.

The determination of the buckling load is through determining the load at which a matrix is singular. Since the matrix becomes singular at multiple values of the loads

(refer to equation 2.3), during the simulations, the computer may miss the lowest buckling load which is most likely the reason for the inconsistencies.

Upon closer examination, we found that warning messages are given for some of the simulations listed in *Table 3.1* and *Table 3.2*. This means that the solution has not converged to the specified 'convergence tolerance' limits. These warning messages could be eliminated by increasing the number of iterations required for the specific simulations gradually. By doing this, we could make the solution to converge accurately and therefore, arrive at the best solution, which, in our case is the critical buckling load. The recalculated results are given in *Table 3.3* and *Table 3.4*. The critical buckling load is plotted against the position of the load application as shown in *Figure 3.4*.

The mode shapes for x = 0.075 in (4^{th} node), 0.25 in (11^{th} node), 0.45 in (19^{th} node), and 0.5 in (21^{st} node) are shown in *Figure3.5*, *Figure 3.6*, *Figure 3.7* and *Figure 3.8* respectively.

Figure 3.5 Buckling mode for load applied at a distance x = 0.075 in (4^{th} node)

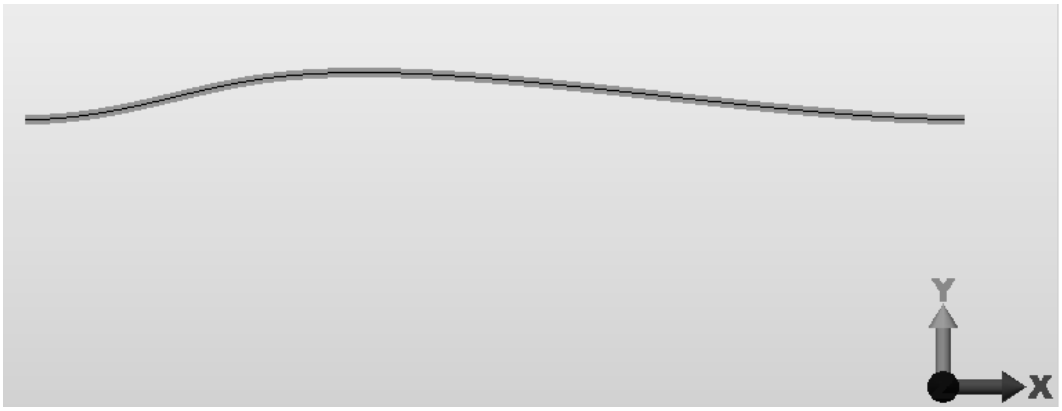

Figure 3.6 Buckling mode for load applied at a distance x = 0.25 in (11th node)

Figure 3.7 Buckling mode for load applied at a distance x = 0.45 in (19th node)

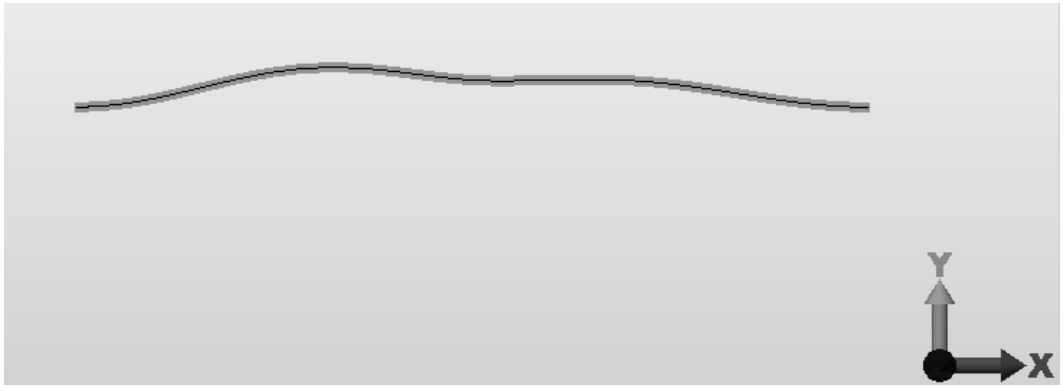

Figure 3.8 Buckling mode for load applied at a distance x = 0.5 in (21st node)

Table 3.3 Results for axial loads for increased number of iterations - 20 elements

Node#	X (in)	Load (Lb-f)	Critical Buckling Load without Warning Message	# of Iterations Used	Critical Buckling Load with Warning Message	# of Iterations Used
1	0	1	Error	32		
2	0.05	1	6182.65	32		
3	0.1	1	3319.05	2000	4010.89	32
5	0.2	1	-1503.70	32		
6	0.25	1	-1309.54	32		
7	0.3	1	-1285.54	32		
8	0.35	1	-1404.44	2000	-1405.26	32
9	0.4	1	1628.71	2000	1629.57	32
10	0.45	1	1683.62	2000	1691.80	32
11	0.5	1	2905.13	32		
12	0.55	1	-1683.62	2000	-1686.32	32
13	0.6	1	-1628.70	2000	-5537.92	32
14	0.65	1	1404.43	2000	1405.84	32
15	0.7	1	1285.54	32		
16	0.75	1	1309.54	32		
17	0.8	1	1503.70	32		
18	0.85	1	2018.15	32		
19	0.9	1	-3319.03	2000	7908.21	32
20	0.95	1	-6182.65	32		
21	1.0	1	Error	32		

Table 3.4 Results for axial loads for increased number of iterations - 40 elements

Node #	X (in)	Load (Lb-f)	Critical Buckling Load without Warning Message	# of Iterations Used	Critical Buckling Load with Warning Message	# of Iterations Used
1	0	1	Error			
4	0.075	1	4259.26	1000	4289.24	32
5	0.1	1	3318.56	1000	12833.8	32
6	0.125	1	-2539.85	1000	-2542.51	32
14	0.325	1	-1326.12	1000	-1326.16	32
15	0.35	1	-1404.23	1000	-1404.78	32
16	0.375	1	-1524.01	1000	-1620.73	32
17	0.4	1	1628.55	1000	2066.54	32
18	0.425	1	1650.27	1000	1654.69	32
19	0.45	1	1683.41	1000	1935.52	32
20	0.475	1	1727.54	1000	1875.68	32
21	0.5	1	-3666.50	32		
22	0.525	1	-1727.54	1000	-1741.18	32
23	0.55	1	-1683.41	1000	-1847.32	32
24	0.575	1	-1650.28	1000	-1650.80	32
25	0.6	1	-1628.55	1000	-1631.21	32
26	0.625	1	1524.01	1000	20493.4	32
27	0.65	1	1404.23	1000	1449.10	32
36	0.875	1	2539.84	1000	2545.78	32
37	0.9	1	-3318.56	1000	12502.0	32

Graphs are plotted for both the 20-element and 40-element beam cases with the position of the load on the X-axis and the buckling load on the Y-axis which are shown in *Figure 3.9.*

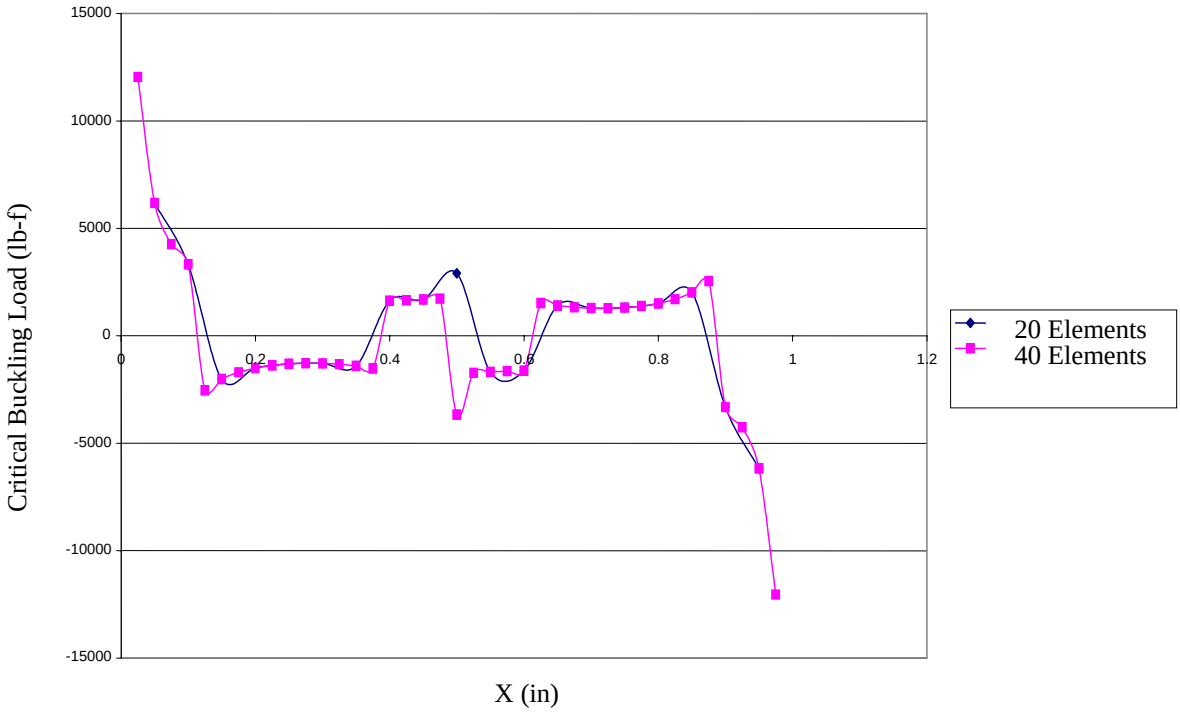

Figure 3.9 Graphs for the 20-element and 40-element beams depicting the variation of the critical buckling load with respect to x for the cases with increased number of iterations

From *Figure 3.9*, we observe that there is a remarkable change in the pattern of the graphs as compared to the one seen in section 3.1.2. Here, from *Figure 3.9*, we see that the graphs for the 20-element and 40-element beam cases have agreed very well with each other as opposed to *Figure3.4* of the previous section, except for the cases where the

axial loads are applied at the midpoint of the beam. At x = 0.5 in, the buckling loads are 2905.13 Lb-f and -3666.50 Lb-f (the negative sign indicates that the buckling occurs in the opposite direction of the current direction of force application) for the 20-element and 40-element beam cases respectively, which is a very huge difference.

3.2 Analysis of a Structure under Thermal Loads

In this part of the analysis, we subject the beam under consideration to thermal loads as shown in *Figure 3.10* and see how the temperature affects the buckling of the beam. The purpose of this study is to learn the correct use of the finite element program since the analytical results can be used to compare with the finite element results.

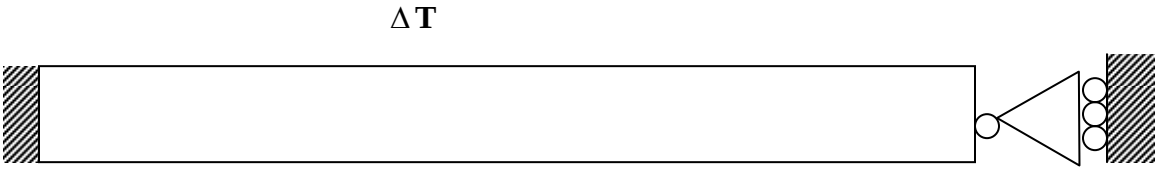

Figure 3.10 Temperature beam

3.2.1 Analysis Procedures

1. Go to the ‘Start menu’ and pull up ‘Programs’, ‘Algor’, ‘Superdraw III’.

2. Go to ‘Add’, ‘Line’ and add a line 8 inches long.

3. Go to ‘Construct’, ‘Divide’ and set the number to, say, 10 and hit the divide button. This will break down your beam into 10 elements.

4. Transfer the model to the ‘FEA Editor’ by going to ‘File, ‘Export to Fempro’.

5. A ‘Units definition’ screen appears. Click ‘OK’ to set it to the default units.

6. Set the ‘Analysis type’ to ‘Critical Buckling Load Analysis’.

7. Set the ‘Element type’ to ‘Beam’.

8. Double click on the ‘Element definition’, highlight any field, say the ‘Area’, click on ‘Cross-section libraries’ and in the top right corner of the dialog box select ‘Rectangular’.

9. Enter the dimensions (b=0.2” and h=0.1”).

10. Click ‘OK’ twice.

11. Set the ‘Material’ to ‘Steel (ASTM-A36)’.

12. Select one of the endpoints of the beam using ‘Vertices-select’ or ‘Rectangular-select’, and constrain all the degrees of freedom of this end.

13. Similarly, select the other end of the beam and constrain the translation of the beam in the x-direction at this end.

14. Now, select the entire beam using ‘Rectangular-select’ and assign a temperature.

Figure 3.11 Beam showing nodal temperatures

15. Go to the ‘Analysis parameters’ window and enter a value of 1 in the ‘Thermal multiplier’ box. This is because we are taking temperature into account in our analysis.
16. Now, after setting up the model, along with the required boundary conditions and loads, click on the ‘Check model’ icon at the top toolbars; this is to run a check to see if everything was done right or not.
17. After checking the model, run the analysis.
18. After the analysis is done, the results of the analysis are displayed in ‘Superview’.
19. Go to the ‘Analysis summary’ in order to obtain the ‘Buckling Load Multiplier’.

3.2.2 Analysis Results and Discussion

The relationship between the critical load of a beam and the critical temperature can be given as the following:

$$P_{cr} = \alpha \Delta T_{cr}\ EA \tag{2.30}$$

where P_{cr} = Critical load of the beam;

α = Co-efficient of thermal expansion of the material of the beam;

ΔT_{cr} = Critical temperature of the beam;

E = Young's modulus of the material of the beam;

A = Cross-sectional area of the beam.

From the above equation, the critical temperature of the beam can be calculated as follows:

$$\Delta T_{cr} = \frac{P_{cr}}{\alpha EA} \tag{2.31}$$

The theoretical calculations for the case at hand are as follows:

From result 2.29, we have P_{cr} = 18.7248 Lb-f.

From equation 2.31, we have

$$\Delta T_{cr} = \frac{P_{cr}}{\alpha EA} = \frac{18.7248 lbf}{6.5\times10^{-6}/°F \times 2.91355\times10^{7} lbf/in^2 \times 0.02 in^2} = 4.9437°F$$

For the different temperatures applied, the corresponding buckling load multipliers obtained from the experiment are given in *Table 3.5*.

Table 3.5 Results for thermal loads

Temperature (^{o}F)	Buckling Load Multiplier (BLM)
20	0.247161
40	0.123580

The Buckling Load Multiplier (BLM) applies to all of the loads that cause buckling. In the thermal model, the load that causes buckling is a temperature difference, namely

DT = Applied nodal temperature – Stress free reference temperature

In our case, we take the stress free reference temperature to be $0°F$.

The beam will buckle at a temperature given by:

$T_{Buckling}$ = Stress free reference temperature + BLM (DT)

= $0°F + 0.247161(20°F - 0°F) = 4.94322°F$ taking the first result of the *Table 3.5* into consideration.

Also, $T_{Buckling}$ = $0°F + 0.123580(40°F - 0°F) = 4.9432°F$ taking the second result of the *Table 3.5* into consideration.

Thus, we see that the theoretical and the experimental values match closely.

For the thermal model studied above, the buckling mode is given by *Figure 3.12.*

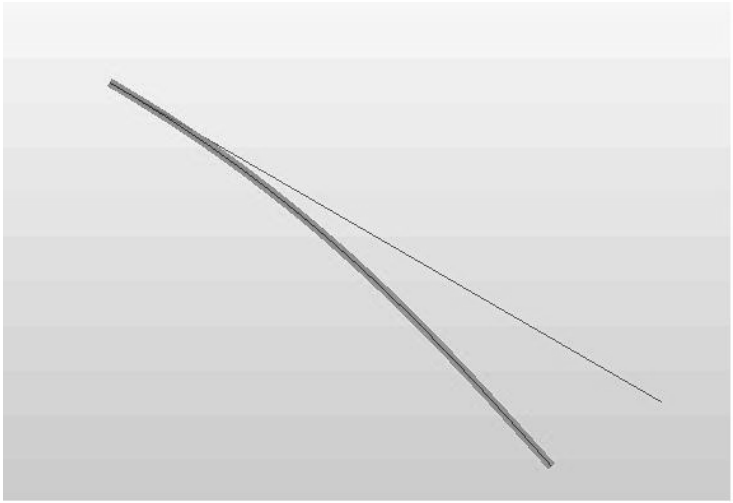

Figure 3.12 Buckling mode

Chapter 4

PLATE BUCKLING ANALYSIS

In this chapter, we examine the effects of various types of loading on the plate elements. We employ the Critical buckling load analysis of the Algor program to thus determine the buckling loads of the plate elements. To understand the phenomenon better, we take localized loads into consideration in this section.

4.1 Geometry and Material Properties of the Plate Element

We consider a plate with geometry given in *Figure 4.1*. The plate has a length of 40 in, breadth of 30 in and a thickness of 0.5 in.

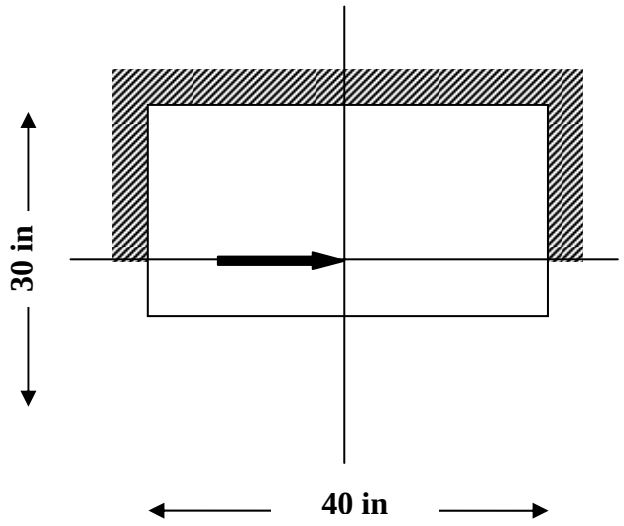

Figure 4.1 Plate geometry showing the loads and boundary conditions

The material properties of the plate are taken to be the same as the ones mentioned in section 2.3.2 of chapter 2 as given in *Table 2.1*.

4.2 Plate Buckling under Axial Loads

4.2.1 Buckling under In-Plane Loads

Here, we subject the plate element to an axial load at its centre to calculate its buckling load.

4.2.1.1 Analysis Procedures

1. Go to the ‘Start menu’ and pull up ‘Programs’, ‘Algor’, ‘Superdraw III’.
2. Go to ‘Add’, ‘Rectangle’ and construct a rectangle of length 40 in and breadth 30 in.
3. Go to ‘FEA Mesh’, ‘Automatic mesh’: ‘4 Point’ and then click on ‘Division values’ and enter the divisions as 20 and 20 in the AB and BC divisions boxes respectively.
4. Then, starting from one of the corners of the rectangle, right click on each of the four corners of the rectangle, in a clock-wise or anti-clockwise manner. By this, we are meshing it.
5. Transfer the model to the ‘FEA Editor’ by going to ‘File’, ‘Export to Fempro’.
6. A ‘Units definition’ screen appears. Click ‘OK’ to set it to the default units.
7. Set the ‘Analysis type’ to ‘Critical Buckling Load’.
8. Set the ‘Element type’ to ‘Plate’.

9. Double click on the ‘Element definition’, and enter the thickness of the plate as 0.5 in.
10. Click ‘OK’.
11. Set the ‘Material type’ to ‘Steel (ASTM-A36)’.
12. Using ‘Rectangular select’, select the vertices of every side of the plate and clamp all the four sides of the plate.
13. Now, select the center point of the plate and enter any value of force in the positive x-direction.
14. Now, after setting up the model, along with the required boundary conditions and loads, click on the ‘Check model’ icon at the top toolbars; this is to run a check to see if everything was done right or not.
15. After checking the model, run the analysis.
16. After the analysis is done, the results of the analysis are displayed in ‘Superview’.
17. Go to the ‘Analysis summary’ in order to obtain the ‘Buckling Load Multiplier’.

4.2.1.2 Analysis Results and Discussion

For the different axial loads applied, the corresponding buckling load multipliers are given in *Table 4.1*. The total buckling load is the product of the applied load and its corresponding buckling load multiplier.

Here, a point load is applied at the center of the plate in the positive X-direction.

Table 4.1 Results for different concentrated loads applied at the center of the plate

Load (Lb-f)	Buckling Load Multiplier
1	6.788812E+06
100	67888.1
200	33944.1
400	16972.0

Hence, the buckling load from the above table is: 100 x 67888.1 = 6788810 Lb-f.

The buckling mode for the plate element is shown in *Figure 4.2*.

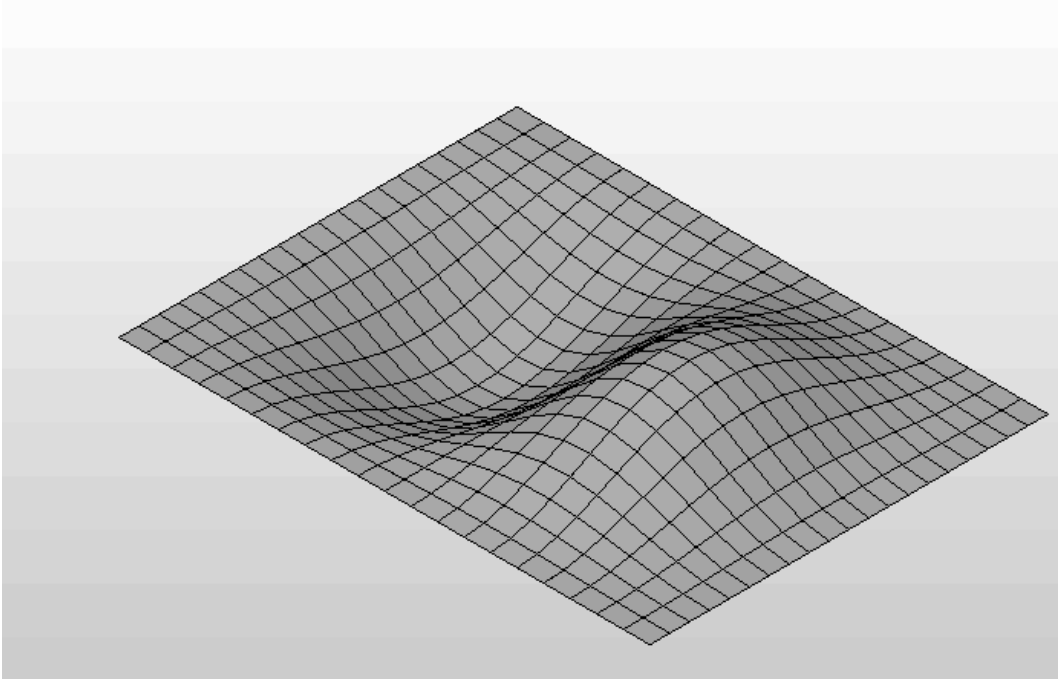

Figure 4.2 Buckling mode

4.2.2 Buckling under Loads applied at Different Nodes along the Midline of the Plate

We apply axial loads to different points within the plate element, along the length of the element and try to observe how the buckling load of the entire plate varies from point to point. See *Figure 4.3 (a)* and *Figure 4.3 (b)* for the loading conditions.

4.2.2.1 Analysis Procedures

The analysis procedure is the same as in section 4.2.1.1 except that here, in addition to the 20 x 20 elements, we also make use of the 40 x 40 elements; and we apply nodal loads to every point or every alternate point of the plate element, as per our requirement. This is illustrated in *Figure 4.3 (a)* and *Figure 4.3 (b)*.

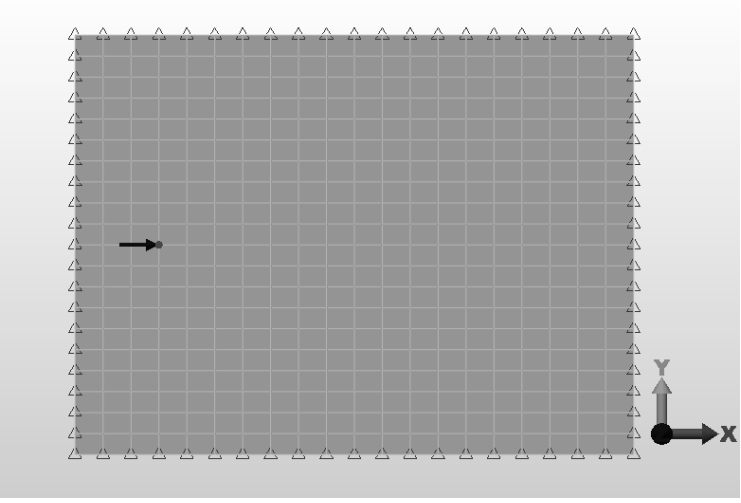

Figure 4.3 (a) Buckling under a concentrated force: Load applied at the 4th node

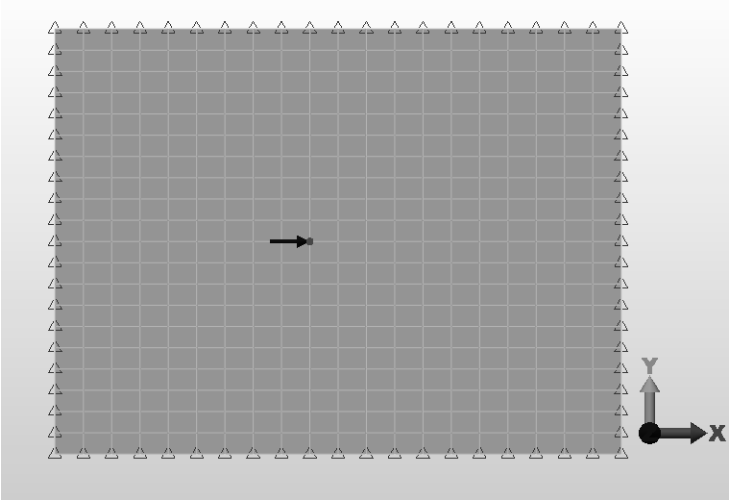

Figure 4.3 (b) Buckling under a concentrated force: Load applied at the 10th node

4.2.2.2 Analysis Results and Discussion

We carried out simulations with the 20x20 plate elements and the 40x40 plate elements respectively. As is the case in chapter 3, we again observe inconsistencies in the critical buckling load which we attributed to the missed modes due to numerical inaccuracies. By increasing the number of iterations, we eliminated the warning messages. The corresponding results are given in *Table 4.2* and *Table 4.3*.

Table 4.2 Results for nodal loads - 20x20 elements

Node#	X (in)	Load (Lb-f)	Critical Buckling Load without Warning Message	# of Iterations Used	Critical Buckling Load with Warning Message	# of Iterations Used
1	0	1	ERROR	32		
2	0.05	1	-3119508	32		

3	0.1	1	-1655051	32		
4	0.15	1	-1371599	32		
5	0.2	1	-1355851	32		
6	0.25	1	-1449403	32		
7	0.3	1	-1517904	1000	-1.615906E+06	32
8	0.35	1	-1465824	32		
9	0.4	1	-1399513	1000	2.836114E+06	32
10	0.45	1	-1361906	1000	-1.759690E+06	32
11	0.5	1	6788812	32		
12	0.55	1	1361897	1000	-3.778746E+07	32
13	0.6	1	1399516	1000	1.408778E+06	32
14	0.65	1	1466014	1000	3.580132E+06	32
15	0.7	1	1517904	1000	1.629562E+06	32
19	0.9	1	1655050	32		
20	0.95	1	3119502	32		
21	1.0	1	ERROR	32		

Table 4.3 Results for nodal loads - 40x40 elements

Node #	X (in)	Load (Lb-f)	Critical Buckling Load without Warning Message	# of iterations	Critical Buckling Load with Warning Message	# of iterations
11	0.25	1	-1407413	1000	-1.407636E+06	32
12	0.275	1	-1450313	1000	-1.451844E+06	32
13	0.3	1	-1459844	1000	-1.481935E+06	32

14	0.325	1	-1437812	1000	-2.126018E+06	32
15	0.35	1	-1404109	1000	-1.550645E+06	32
16	0.375	1	-1371404	1000	-1.438150E+06	32
17	0.4	1	-1344506	1000	-1.793890E+06	32
18	0.425	1	-1324894	1000	-1.561724E+06	32
19	0.45	1	-1312830	1000	-2.474154E+06	32
20	0.475	1	-1308379	1000	-9.131377E+06	32
21	0.5	1	-2163315	32		
22	0.525	1	1308386	1000	6.079460E+06	32
23	0.55	1	1312833	1000	2.430052E+06	32
24	0.575	1	1324896	1000	1.817019E+06	32
25	0.6	1	1344510	1000	1.590213E+06	32
26	0.625	1	1371402	1000	2.166104E+06	32
27	0.65	1	1404109	1000	1.801099E+06	32
28	0.675	1	1437815	1000	1.556229E+06	32
29	0.7	1	1459845	1000	1.630440E+06	32
30	0.725	1	1450311	1000	1.500710E+06	32

Again, a graph is plotted with the so obtained results as shown in *Figure 4.4.*

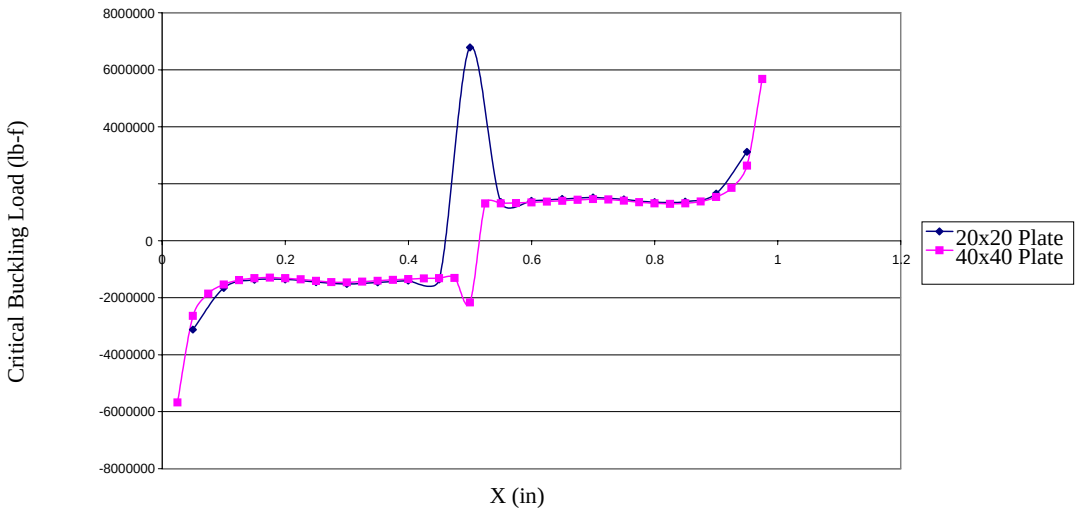

Figure 4.4 Graphs for the 20x20 elements plate and the 40x40 elements plate depicting the variation of the critical buckling load with respect to x for the cases with increased number of iterations

From *Figure 4.4*, we see that exactly similar to the graph obtained in section 3.1.3 of chapter 3, the graphs corresponding to the 20x20 plate element and the 40x40 plate elements agree almost very well with each other except for the cases when the load is acting at the midpoint of the plate. At x = 0.5 in, the critical buckling load is 6788812 Lb-f for the 20x20 plate and it is -2163315 Lb-f for the 40x40 plate, which shows that there is again a large difference in the magnitudes of the forces.

Four representative mode shapes for the 20x20 and the 40x40 plates for x = 0.5 in (20x20 plate, 11^{th} node), 0.275 in (40x40 plate, 12^{th} node), 0.475 in (40x40 plate, 20^{th} node), and 0.5 in (40x40 plate, 21^{st} node) are shown in *Figure 4.5*, *Figure 4.6*, *Figure 4.7* and *Figure 4.8* respectively.

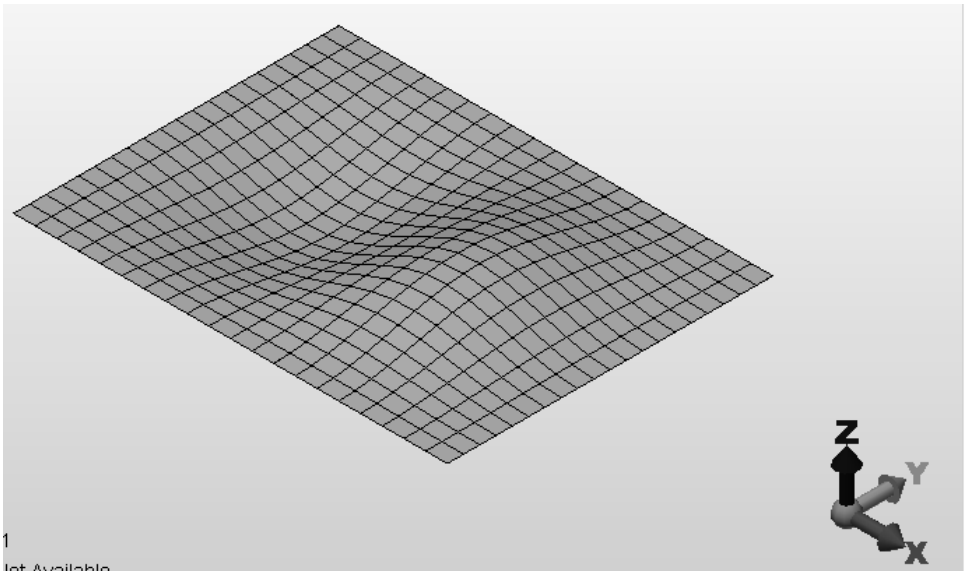

Figure 4.5 Buckling mode of a 20x20 plate for a load applied at the 11th node

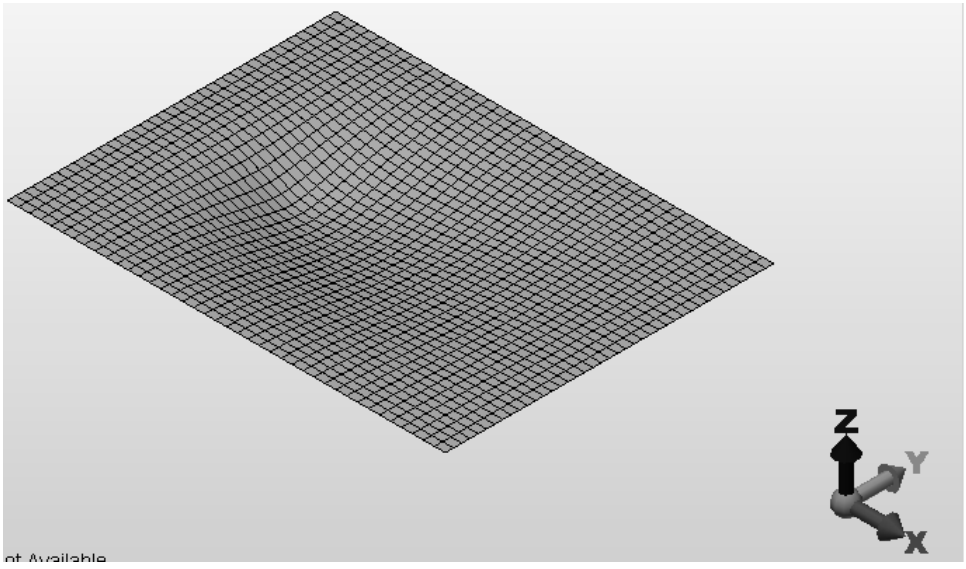

Figure 4.6 Buckling mode of a 40x40 plate for a load applied at the 12th node

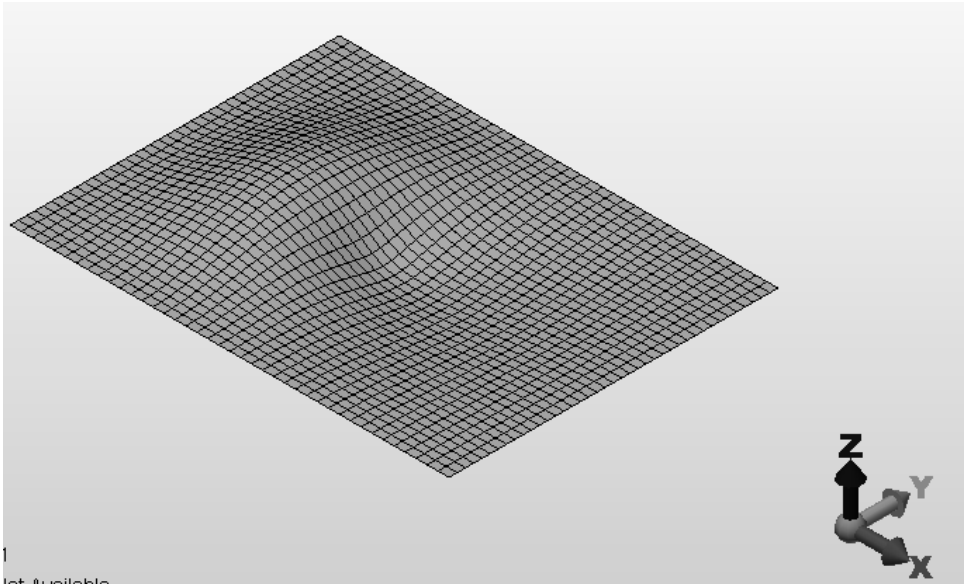

Figure 4.7 Buckling mode of a 40x40 plate for a load applied at the 20th node

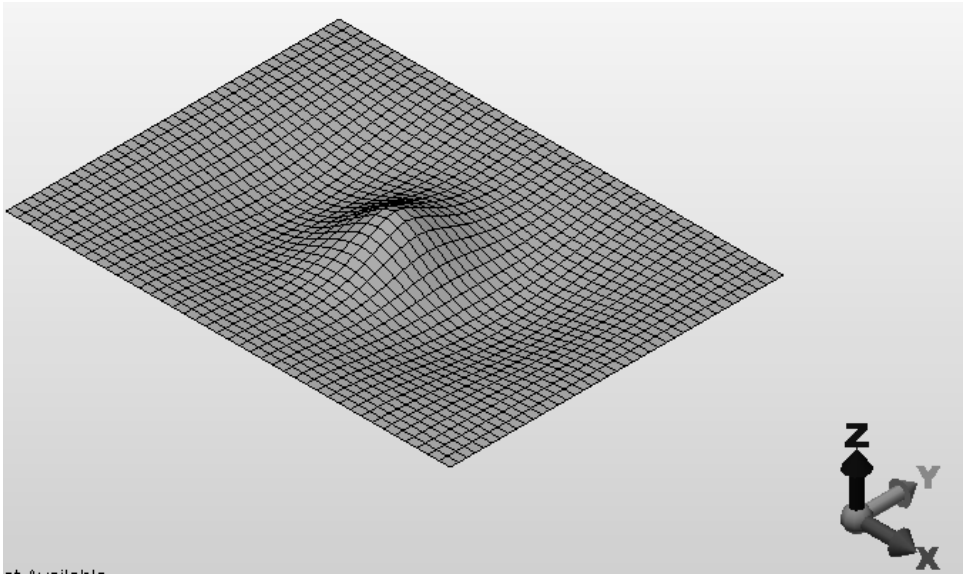

Figure 4.8 Buckling mode of a 40x40 plate for a load applied at the 21st node

4.2.3 Buckling under Localized Loads - Local In-Plane Load

We examine the case where a plate element is subjected to equal and opposite loads to calculate the resultant buckling load as shown in *Figure 4.9*.

4.2.3.1 Analysis Procedures

1. Go to the ‘Start menu’ and pull up ‘Programs’, ‘Algor’, ‘Superdraw III’.
2. Go to ‘Add’, ‘Rectangle’ and construct a rectangle of length 40 in and breadth 30 in.
3. Go to ‘FEA Mesh’, ‘Automatic mesh’: ‘4 Point’ and then click on ‘Division values’ and enter the divisions as 20 and 20 in the AB and BC divisions boxes respectively.
4. Then, starting from one of the corners of the rectangle, right click on each of the four corners of the rectangle, in a clock-wise or anti-clockwise manner. By this, we are meshing it.
5. Transfer the model to the ‘FEA Editor’ by going to ‘File’, ‘Export to Fempro’.
6. A ‘Units definition’ screen appears. Click ‘OK’ to set it to the default units.
7. Set the ‘Analysis type’ to ‘Critical Buckling Load’.
8. Set the ‘Element type’ to ‘Plate’.
9. Double click on the ‘Element definition’, and enter the thickness of the plate as 0.5 in.
10. Click ‘OK’.
11. Set the ‘Material type’ to ‘Steel (ASTM-A36)’.
12. Using ‘Rectangular select’, select the vertices of every side of the plate and clamp

all the four sides of the plate.

13. Now, select some two random points within the plate, and enter the same values of forces at these two points, one force in the positive x-direction and the other force in the negative x-direction as shown in *Figure 4.9*.

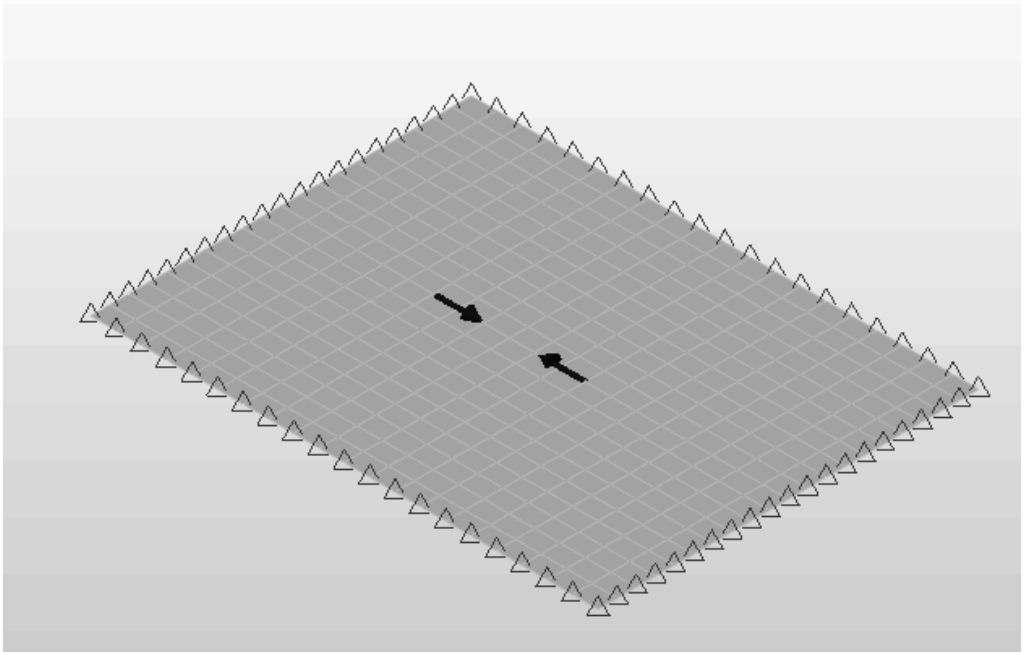

Figure 4.9 Plate element with two equal and opposite forces applied at two random points

14. Now, after setting up the model, along with the required boundary conditions and loads, click on the ‘Check model’ icon at the top toolbars; this is to run a check to see if everything was done right or not.
15. After checking the model, run the analysis.
16. After the analysis is done, the results of the analysis are displayed in ‘Superview’.

17. Go to the ‘Analysis summary’ in order to obtain the ‘Buckling Load Multiplier’.

4.2.3.2 Analysis Results and Discussion

For the different axial loads applied, the corresponding buckling load multipliers are given in the *Table 4.4*.

Table 4.4 Results for the dual-load plate element

Loads applied at two random points within the plate (Lb-f)	Buckling Load Multiplier
1	935147
100	9351.47
200	4675.74
400	2337.87

The load which theoretically causes buckling is equal to each and every load multiplied by the buckling load multiplier. In this case with the opposing loads, the plate will buckle when both the loads are each 935,147 Lb-f.

The buckling mode for this case is shown in *Figure 4.10*.

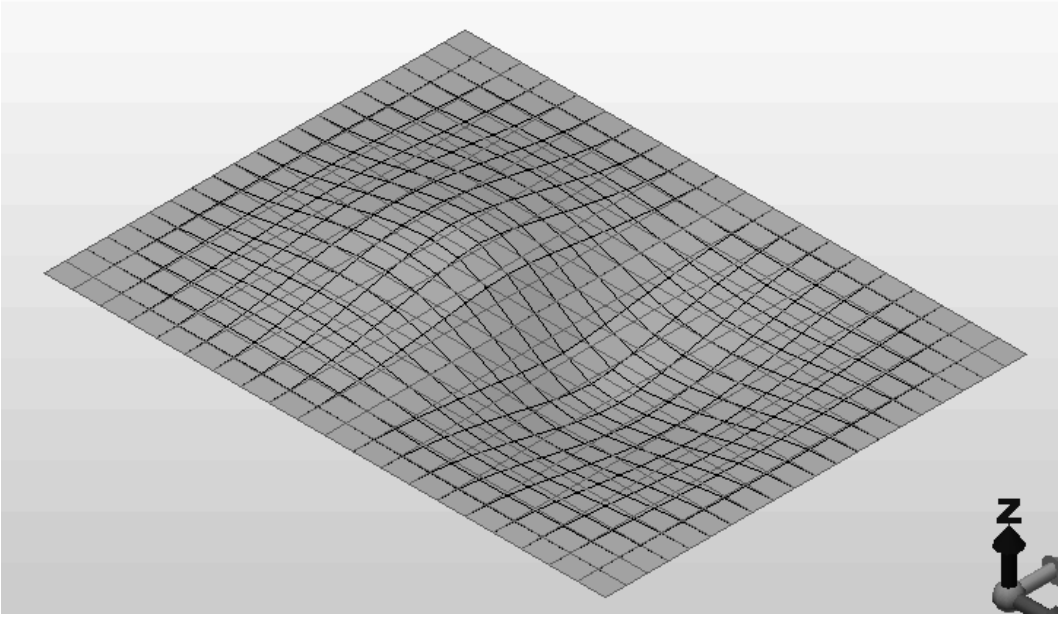

Figure 4.10 Buckling mode

4.3 Plate Buckling under Thermal Loads

All through we had dealt with only force loads. We now introduce temperature loads in order to study the effects of temperature on the buckling of the plate element.

4.3.1 Buckling under Uniform Thermal Load

We first consider the case of a uniform temperature applied to the entire plate element where the critical temperature of the plate can be calculated.

4.3.1.1 Analysis Procedures

The analysis procedures are the same as the ones mentioned in section 4.2.1.1 till step 12. The next few steps are as follows:

13. Now, select the entire plate using ‘Rectangular-select’ and assign a temperature. The plate element shown in *Figure 4.11* shows the nodal temperatures.

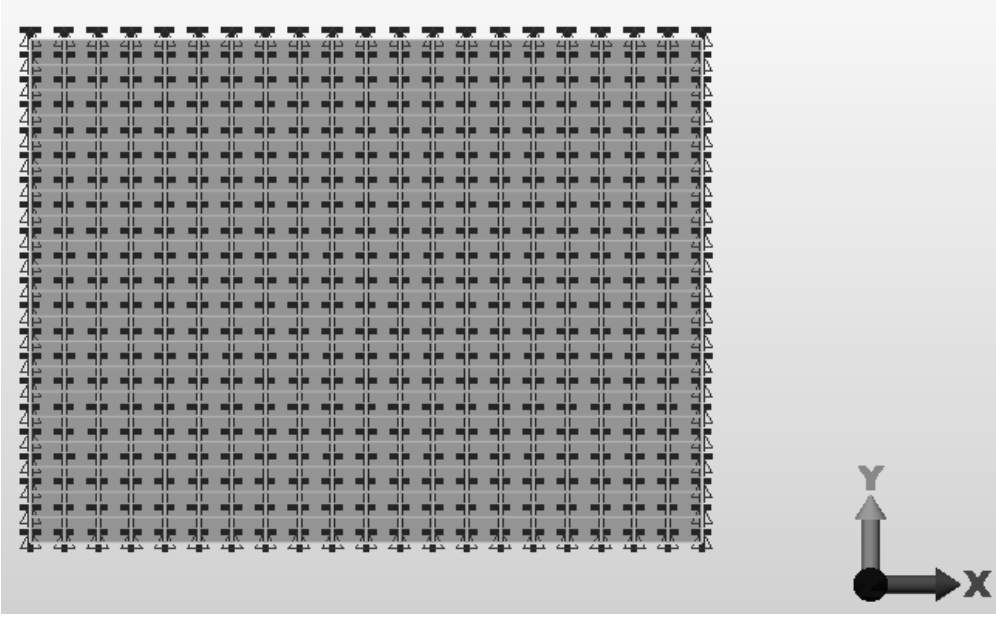

Figure 4.11 Plate element showing uniform nodal temperatures

14. Go to the ‘Analysis parameters’ window and enter a value of 1 in the ‘Thermal multiplier’ box. This is because we are taking temperature into account in our analysis.
15. Now, after setting up the model, along with the required boundary conditions and

loads, click on the ‘Check model’ icon at the top toolbars; this is to run a check to see if everything was done right or not.

16. After checking the model, run the analysis.
17. After the analysis is done, the results of the analysis are displayed in ‘Superview’.
18. Go to the ‘Analysis summary’ in order to obtain the ‘Buckling Load Multiplier’.

4.3.1.2 Analysis Results and Discussion

For the different values of temperatures applied to the plate element, a set of buckling load multiplier values are obtained from the simulation that is shown in *Table 4.5*.

Table 4.5 Results for uniform temperature plate

Temperature (^{o}F)	Buckling Load Multiplier (BLM)
20	5.94241
50	2.37696
100	1.18848

The Buckling Load Multiplier (BLM) applies to all of the loads that cause buckling. In the thermal model, the load that causes buckling is a temperature difference, namely,

DT = Applied nodal temperature – Stress free reference temperature

In our case, we take the stress free reference temperature to be $0°F$.

The plate will buckle at a temperature given by:

$T_{Buckling}$ = Stress free reference temperature + BLM (DT)

= $0°F + 5.94241(20°F - 0°F) = 118.8482°F$ taking the first result of the *Table 4.5* into consideration.

Also, $T_{Buckling} = 0°F + 2.37696(50°F - 0°F) = 118.848°F$ taking the second result of the *Table 4.5* into consideration.

4.3.2 Buckling under Localized Loads - Local Temperature Load

In this section, we consider localized temperature loads. This concept is implemented by subjecting a single plate element to two different temperatures in two different regions. Our intention here is to see how the temperature changes bring about changes in the buckling patterns of the element, which would prove to be an important study.

4.3.2.1 Analysis Procedures

1. Go to the ‘Start menu’ and pull up ‘Programs’, ‘Algor’, ‘Superdraw III’.
2. Go to ‘Add’, ‘Rectangle’ and construct a rectangle of length 40 in and breadth 30 in.
3. Go to ‘FEA Mesh’, ‘Automatic mesh’: ‘4 Point’ and then click on ‘Division values’ and enter the divisions as 20 and 20 in the AB and BC divisions boxes respectively.
4. Then, starting from one of the corners of the rectangle, right click on each of the

four corners of the rectangle, in a clock-wise or anti-clockwise manner. By this, we are meshing it.

5. Transfer the model to the ‘FEA Editor’ by going to ‘File’, ‘Export to Fempro’.
6. A ‘Units definition’ screen appears. Click ‘OK’ to set it to the default units.
7. Set the ‘Analysis type’ to ‘Critical Buckling Load’.
8. Set the ‘Element type’ to ‘Plate’.
9. Double click on the ‘Element definition’, and enter the thickness of the plate as 0.5 in and in the box named as ‘Temperature method’, change the option to ‘Nodal dT’, as we will use temperatures in this particular analysis.
10. Click ‘OK’.
11. Set the ‘Material type’ to ‘Steel (ASTM-A36)’.
12. Using the ‘Rectangular-select’ option, select the vertices of every side of the plate and clamp all the four sides of the plate for the clamped boundary conditions and similarly, constrain the necessary translations and rotations of the sides of the plate for the simply-supported boundary conditions.
13. Now, select the entire plate using the ‘Rectangular-select’, and then apply the required temperature to it.
14. Next, select a small center patch within the plate and apply a temperature higher to it than the rest of the plate.
15. Double click on the ‘Analysis parameters’ and enter a value of 1 in the ‘Thermal multiplier’ box, since we are taking temperatures into account.

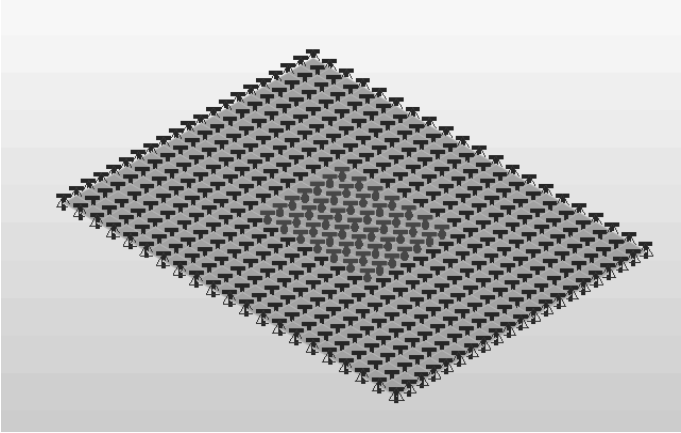

Figure 4.12 Plate element showing two different sets of nodal temperatures – one set of temperatures correspond to the center patch and the other of the region around it

16. Now, after setting up the model, as shown in *Figure 4.11*, along with the required boundary conditions and temperatures, click on the 'Check model' icon at the top toolbars; this is to run a check to see if everything was done right or not.
17. After checking the model, run the analysis.
18. After the analysis is done, the results of the analysis are displayed in 'Superview'.
19. Go to the 'Analysis summary' in order to obtain the 'Buckling Load Multiplier'.

4.3.2.2 Analysis Results

The results for the clamped and simply-supported boundary conditions are given in *Table 4.5* and *Table 4.6* respectively.

Table 4.6 Results for critical buckling load analysis for Clamped boundary conditions

Outside Plate Temperature (^{o}F)	Center Patch Temperature (^{o}F)	Buckling Load Multiplier Value
0	50	8.41206
0	100	4.20603
20	70	3.53163
20	20	5.94241

Table 4.7 Results for critical buckling load analysis for Simply-supported boundary conditions

Outside Plate Temperature (^{o}F)	Center Patch Temperature (^{o}F)	Buckling Load Multiplier Value
0	50	4.20992
0	100	2.10496
20	70	1.43089
20	20	2.13492

The buckling mode for a clamped plate with a uniform temp of 20 deg F is shown in *Figure 4.12*.

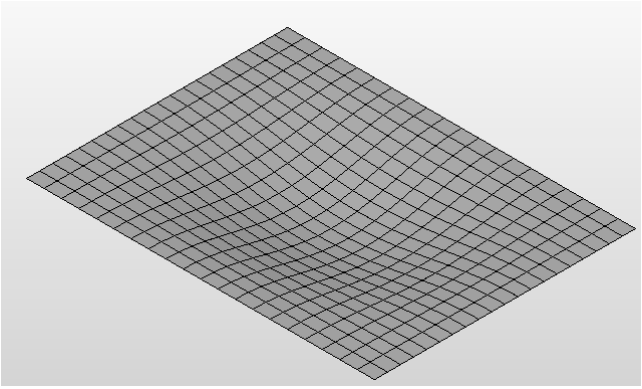

Figure 4.13 Buckling mode

Chapter 5

EFFECT OF IN-PLANE STRESS ON BEAM AND PLATE VIBRATION

The buckling analysis results obtained in the previous two chapters are still inconsistent even when a large number of iterations have been used in the simulations. For example, for the beam element, the critical buckling loads are 2905.13 Lb-f for the 20-element beam and -3666.50 Lb-f for the 40-element beam. For the plate element, we obtain the critical buckling loads as 6788812 Lb-f for the 20x20 plate and -2163315 Lb-f for the 40x40 plate.

Although we strongly suspect that these inconsistencies are caused by the failure of the Algor program to detect the lowest buckling modes, we would like to show that vibration characteristics, namely the modal frequencies can be used as another indication for the occurrence of buckling. In this chapter, we employ the 'Natural frequency (modal) analysis with load stiffening'. This analysis determines a part's natural frequencies and mode shapes and accounts for the imposed loads when calculating the natural frequencies and mode shapes. It can determine if a part resonates at the frequency of an attached, power-driven device, such as a motor.

5.1 Beam Frequencies

5.1.1 Geometry and Material Properties of the Beam

The geometry and material properties of the beam element under consideration are the same as the ones mentioned in section 2.3.2 of chapter 2, as given in *Figure 2.5* and in *Table 2.1* respectively.

5.1.2 Analysis of a Cantilever Beam under an Axial Load at the Free End

We have seen in section 2.3.3 of chapter 2 where we apply an axial load to the beam element and run the 'Critical buckling load analysis' and obtain a value of 18.6359 Lb-f as the critical load of the beam through the algor simulation. We introduce this section here as an effort to validate the results obtained in section 2.3.3 by subjecting the same beam element to the 'Natural frequency with load stiffening' analysis.

5.1.2.1 Analysis Procedures

The analysis procedure is the same as the one mentioned in section 2.3.3.1 up to step 12

except that, in step 6, we use the 'Natural frequency with load stiffening' analysis instead of the 'Critical buckling load' analysis. The next steps are as follows:

13. Apply a random value of load axially at the free end of the beam in the negative x direction and run the analysis.
14. Make a note of the frequencies obtained.
15. Apply another load and do the same.
16. Compare the frequencies obtained and try to apply loads in such a way that the frequency of the first mode goes down to almost zero.

5.1.2.2 Analysis Results and Discussion

The beam frequencies for the first five modes for various loads applied at the free end of the beam are shown in *Table 5.1*.

Table 5.1 Beam frequencies with different axial loads

Force at the free end of the beam in the negative x-direction (Lb-f)	Mode # 1	Mode # 2	Mode # 3	Mode # 4	Mode # 5
1	48.6432	99.1568	307.748	616.344	854.969
2	47.3352	98.5271	306.369	615.658	853.817
4	44.5739	97.252	303.589	614.282	851.507
6	41.5843	95.9553	300.782	612.904	849.192
8	38.3104	94.6362	297.946	611.522	846.871
10	34.6686	93.2937	295.083	610.137	844.545
12	30.5237	91.9265	292.19	608.748	842.212
14	25.6278	90.5336	289.268	607.356	839.874
15	22.7484	89.8271	287.796	606.658	838.702
16	19.4144	89.1137	286.316	605.96	837.529
17	15.3309	88.3932	284.829	605.261	836.355
18	9.58158	87.6654	283.334	604.561	835.179

18.2	7.93695	87.519	283.034	604.421	834.944
18.3	6.96911	87.4456	282.883	604.351	834.826
18.4	5.8419	87.3722	282.733	604.281	834.709
18.45	5.18673	87.3355	282.658	604.246	834.65
18.5	Error				

Using the results from *Table 5*.1, graphs are plotted between the loads applied and the respective frequencies obtained for the first three modes as shown in *Figure 5*.1. Another set of graphs are plotted between the loads applied and the respective squares of the frequencies, also for the first three modes as shown in *Figure 5.2*.

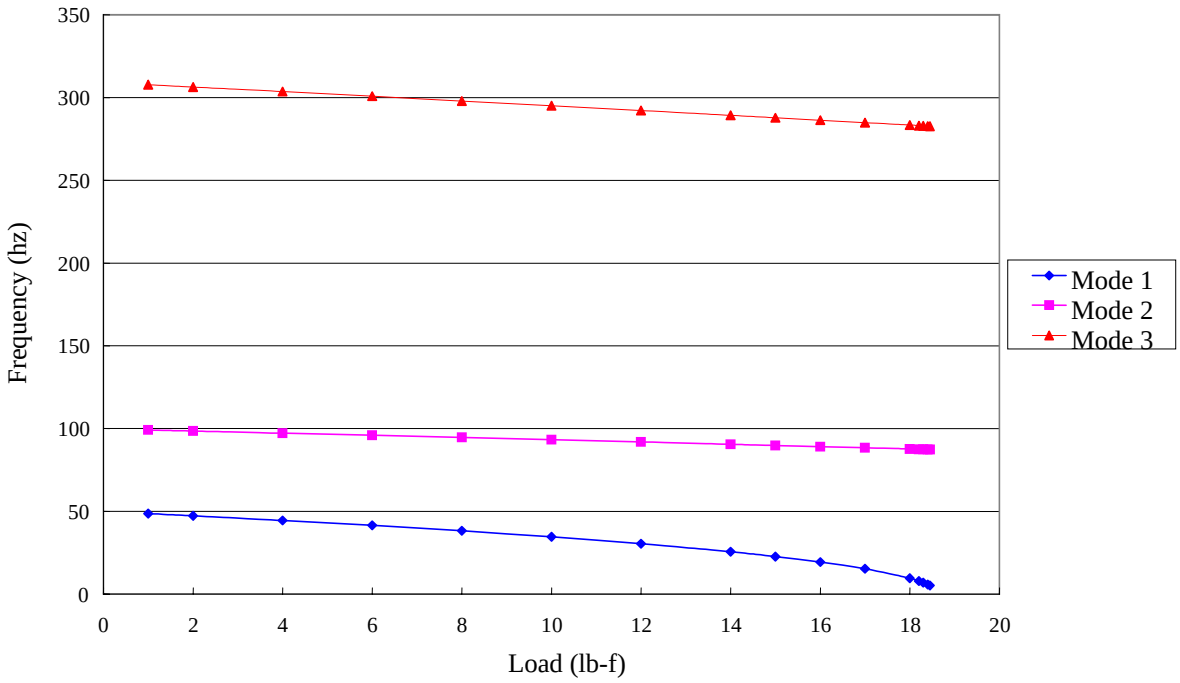

Figure 5.1 Plot between loads and frequencies showing the first 3 modes of the beam

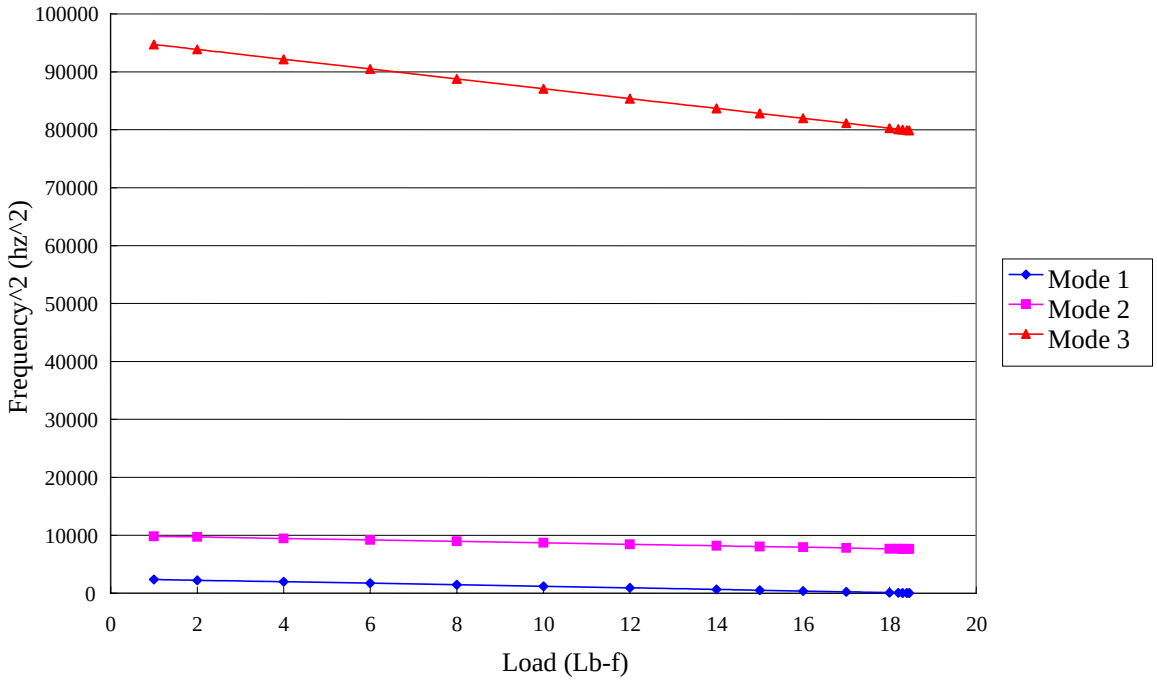

Figure 5.2 Plot between loads and squares of the frequencies showing the first 3 modes of the beam

From the results shown in *Table 5.1*, it is seen that the frequency of the beam is the lowest for 18.45 Lb-f load. This load at which the frequency becomes the lowest or goes almost to zero corresponds to the critical buckling load of the beam. In section 2.3.3.2, the critical buckling load obtained from the 'Critical buckling load' analysis is 18.6359 Lb-f which is quite near to the value obtained from the 'Natural frequency with load stiffening' analysis. Since the results of both these analyses almost agree with each other, it can be as well be stated that the 'Natural frequency with load stiffening' analysis can be used as an alternative method to arrive at buckling loads. From *Figure 5.2*, we see that the graphs between the forces and the squares of frequencies follow a linear relationship.

5.1.3 Analysis of a Beam under Nodal Loads

In section 3.1 of chapter 3, we apply nodal loads to a clamped-clamped beam along its length at various points and calculate the corresponding buckling loads using the 'Critical buckling load' analysis. Here, in this section, we make use of the same beam element and apply a set of loads at its center and run the 'Natural frequency with load stiffening' analysis to determine the buckling load in an attempt to see if these analyses agree with each other again for the case at hand.

We deal with two cases here – (i) when the beam is divided into 20 elements; and (ii) when the beam is divided into 40 elements. The increased number of elements is only an attempt to obtain greater accuracy.

5.1.3.1 Analysis Procedures

1. Go to the 'Start menu' and pull up 'Programs', 'Algor', 'Superdraw III'.
2. Go to 'Add', 'Line' and add a line 8 inches long.
3. Go to 'Construct', 'Divide' and set the number to, say, 20 (or 40) and hit the divide button. This will break down your beam into 20 (or 40) elements.
4. Transfer the model to the 'FEA Editor' by going to 'File', 'Export to Fempro'.
5. A 'Units definition' screen appears. Click 'OK' to set it to the default units.
6. Set the 'Analysis type' to 'Natural Frequency with Load Stiffening'.
7. Set the 'Element type' to 'Beam'.
8. Double click on the 'Element definition', highlight any field, say the area, press on

‘Cross-section libraries’ and in the top right corner of the dialog box select ‘Rectangular’.

9. Enter the dimensions (b=0.2” and h=0.1”).
10. Click ‘OK’ twice.
11. Set the ‘Material’ to ‘Steel (ASTM-A36)’.
12. Select both the endpoints of the beam using ‘Vertices-select’ or ‘Rectangular- select’, and constrain all the degrees of freedom.
13. Apply a random value of load axially at the midpoint of the beam in the positive x-direction and run the analysis.
14. Make a note of the frequencies obtained.
15. Apply another load and do the same.
16. Compare the frequencies obtained and try to apply loads in such a way that the frequency of the first mode goes down to almost zero.

5.1.3.2 Analysis Results and Discussion

The beam frequencies for the first five modes obtained for various loads applied at the midpoint of the 20-element beam are shown in *Table 5.2*.

Table 5.2 Beam frequencies for 20-element beam

Load (Lb-f)	Mode#1	Mode#2	Mode#3	Mode#4	Mode#5
500	312.938	634.881	846.835	1719.09	2821.15
1000	291.396	632.726	753.797	1719.07	2787.23
1500	224.596	594.686	629.05	1706.06	2737.83
1700	138.303	514.778	627.125	1693.81	2715.86
1750	89.1704	494.509	626.601	1689.9	2710.31
1770	54.7011	486.485	626.387	1688.24	2708.09
1780	20.0203	482.499	626.278	1687.38	2706.98
2200	349.253	426.452	621.069	1635.96	2661.67
2300	326.392	492.342	619.629	1618.63	2651.64
2500	282.25	612.138	616.499	1577.18	2632.99
3000	87.0509	607.072	864.454	1429.36	2596.17
3025	55.5475	606.534	875.834	1420.2	2594.72
3030	46.5935	606.426	878.099	1418.35	2594.43
3040	18.0331	606.209	882.618	1414.63	2593.86

Using the results from *Table 5.2*, graphs are plotted between the loads applied and the respective frequencies obtained for the first three modes as shown in *Figure 5.3*. Another set of graphs are plotted between the loads applied and the respective squares of the frequencies, also for the first three modes as shown in *Figure 5.4*.

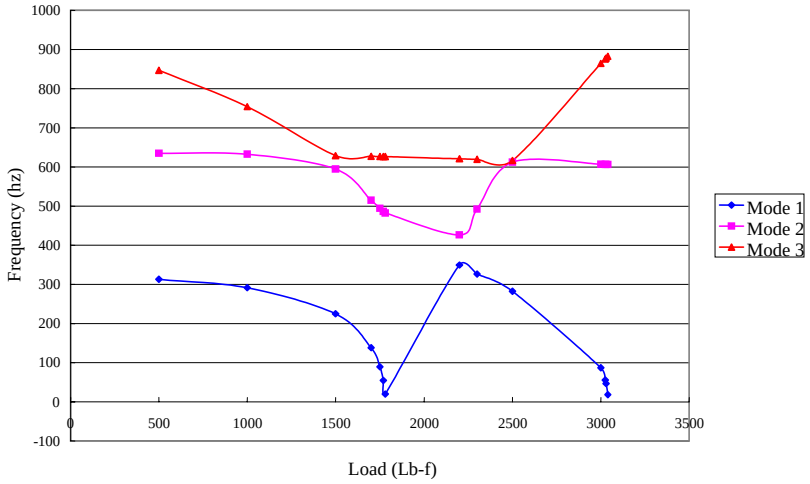

Figure 5.3 Graph between loads and frequencies of a 20-element beam showing the first 3 modes

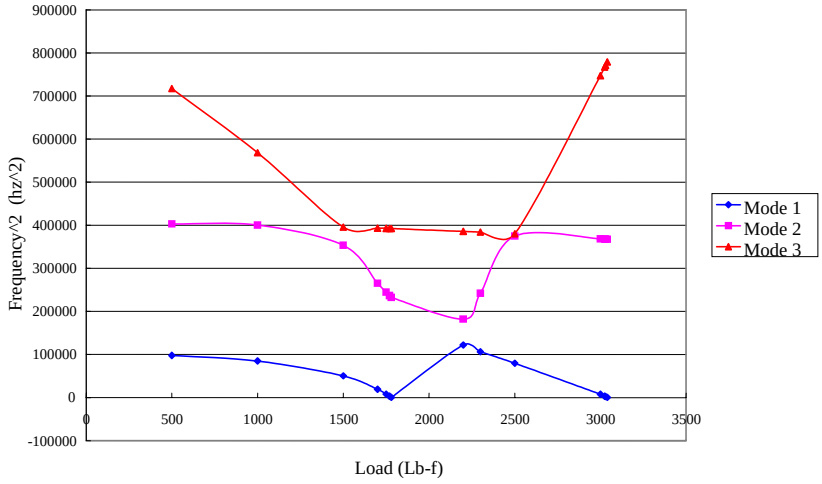

Figure 5.4 Graph between loads and squares of the frequencies of a 20-element beam showing the first 3 modes

Table 5.2 indicates that the beam comprising 20 elements has the least frequency when a load of 3040 Lb-f is applied to it at its center. In other words, this is the critical buckling load of the beam according to the 'Natural frequency with load stiffening' analysis. But, the critical buckling load as obtained from the 'Critical buckling load' analysis for the same case is 2905.13 Lb-f which, though not exactly near the 'Natural frequency with load stiffening' analysis value, is somewhat close.

The beam frequencies for the first five modes obtained for various loads applied at the midpoint of the 40-element beam are shown in *Table 5.3*.

Table 5.3 Beam frequencies for a 40-element beam

Load (Lb-f)	Mode#1	Mode#2	Mode#3	Mode#4	Mode#5
500	312.936	634.885	846.856	1719.27	2822.08
750	304.822	633.991	808.271	1720.02	2807.54
1000	291.383	632.728	753.795	1719.2	2788.13
1250	268.648	631.086	682.698	1715.19	2764.79
1500	224.535	594.613	629.048	1706.1	2738.66
1600	192.342	555.253	628.118	1700.59	2727.73
1700	138.104	514.659	627.121	1693.81	2716.64
1750	88.7944	494.38	626.596	1689.89	2711.08
1770	54.0353	486.351	626.382	1688.22	2708.85
1775	40.4	484.355	626.328	1687.79	2708.29
1776	37.0453	483.956	626.317	1687.71	2708.18
1777	33.3435	483.557	626.306	1687.62	2708.07

Using the results from *Table 5.3*, graphs plotted between the loads applied and the respective frequencies obtained for the first three modes are shown in *Figure 5.5* while another set of graphs plotted between the loads applied and the respective squares of the frequencies, also for the first three modes are shown in *Figure 5.6*.

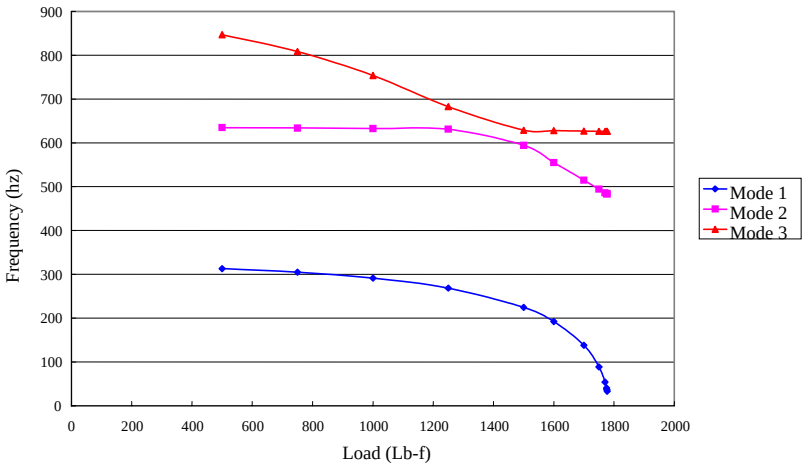

Figure 5.5 Graph between loads and frequencies of a 40-element beam showing the first 3 modes

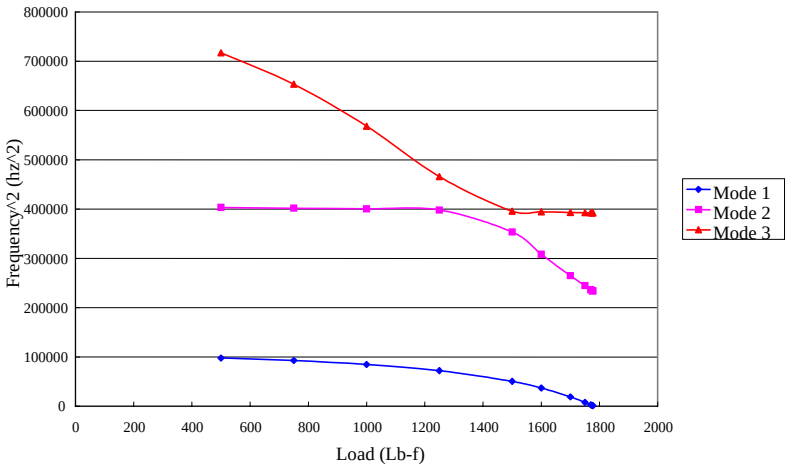

Figure 5.6 Graph between loads and squares of the frequencies of a 40-element beam showing the first 3 modes

Table 5.3 gives the frequencies for various loads applied at the midpoint of the beam which is divided into 40 elements. It indicates that the buckling load is 1777 Lb-f (load corresponding to the least frequency value) but the result obtained from the 'Critical buckling load' analysis for the same case is -3666.50 Lb-f which is not in agreement with the result obtained from the 'Natural frequency with load stiffening' analysis.

5.2 Plate Frequencies

5.2.1 Geometry and Material Properties of the Plate

The geometry and material properties of the plate element under consideration are the same as those discussed in section 4.1 of chapter 4, except that, in this section, we use an additional geometry of the plate element in which we take the breadth of the plate to be 20 in instead of 30 in for some cases.

5.2.2 Analysis of a Plate under Uniform Thermal Loads

In this section, we try to validate the results that have been obtained from the 'Critical buckling load' analysis for the case of a plate with uniform thermal loads.

5.2.2.1 Analysis Procedures

1. Go to the ‘Start menu’ and pull up ‘Programs’, ‘Algor’, ‘Superdraw III’.
2. Go to ‘Add’, ‘Rectangle’ and construct a rectangle of length 40 in and breadth 30 in or of length 40 in and breadth 20 in as required.
3. Go to ‘FEA Mesh’, ‘Automatic mesh’, ‘4 Point’ and then click on ‘Division values’ and enter the divisions as 20 and 20 in the AB and BC divisions boxes respectively.
4. Then, starting from one of the corners of the rectangle, right click on each of the four corners of the rectangle, in a clock-wise or anti-clockwise manner. By this, we are meshing it.
5. Transfer the model to the ‘FEA Editor’ by going to ‘File’, ‘Export to Fempro’.
6. A ‘Units definition’ screen appears. Click ‘OK’ to set it to the default units.
7. Set the ‘Analysis type’ to ‘Natural Frequency (Modal) with Load Stiffening’.
8. Set the ‘Element type’ to ‘Plate’.
9. Double click on the ‘Element definition’, and enter the thickness of the plate as 0.5 in and in the box named as ‘Temperature method’, change the option to ‘Nodal dt’, as we will use temperatures in this particular analysis.
10. Click ‘OK’.
11. Set the ‘Material type’ to ‘Steel (ASTM-A36)’.
12. Using the ‘Rectangular-select’ option, select the vertices of every side of the plate and clamp all the four sides of the plate for the clamped boundary conditions and similarly, constrain the necessary translations and rotations of the sides of the plate for the simply-supported boundary conditions.

13. Now, select the entire plate using the rectangular select, and then apply the required temperature to it.
14. Double click on the ‘Analysis parameters’ and enter a value of 1 in the ‘Thermal multiplier’ box, since we are taking temperatures into account.
15. Now, after setting up the model, along with the required boundary conditions and temperatures, click on the ‘Check model’ icon at the top toolbars; this is to run a check to see if everything was done right or not.
16. After checking the model, run the analysis.
17. After the analysis is done, the results of the analysis are displayed in ‘Superview’.
18. Record the first five natural frequency values that are displayed in the ‘Superview’.

5.2.2.2 Analysis Results and Discussion

The frequencies of the first five modes for the plate geometry 40 in x 30 in x 0.5 in for the clamped boundary conditions are shown in *Table 5.4*.

Table 5.4 Frequencies for a 40 in x 30 in x 0.5 in plate for clamped boundary conditions

Temperature (^{o}F)	Mode#1	Mode#2	Mode#3	Mode#4	Mode#5
0	152.323	256.085	358.483	426.679	455.702
20	139.288	241.029	343.607	410.87	440.06

40	124.761	224.889	328.007	394.401	423.803
50	116.761	216.335	319.902	385.892	415.421
60	108.122	207.405	311.572	377.185	406.854
80	88.1508	188.191	294.157	359.116	389.121
100	61.6335	166.64	275.572	340.061	370.488
120	15.306	141.671	255.559	319.847	350.81
120.25	16.8855	141.33	255.298	319.586	350.556
120.5	18.3296	140.988	255.037	319.325	350.303

Using the results from *Table 5.4*, graphs are plotted between the applied temperatures and obtained frequencies for the first five modes as shown in *Figure 5.7*.

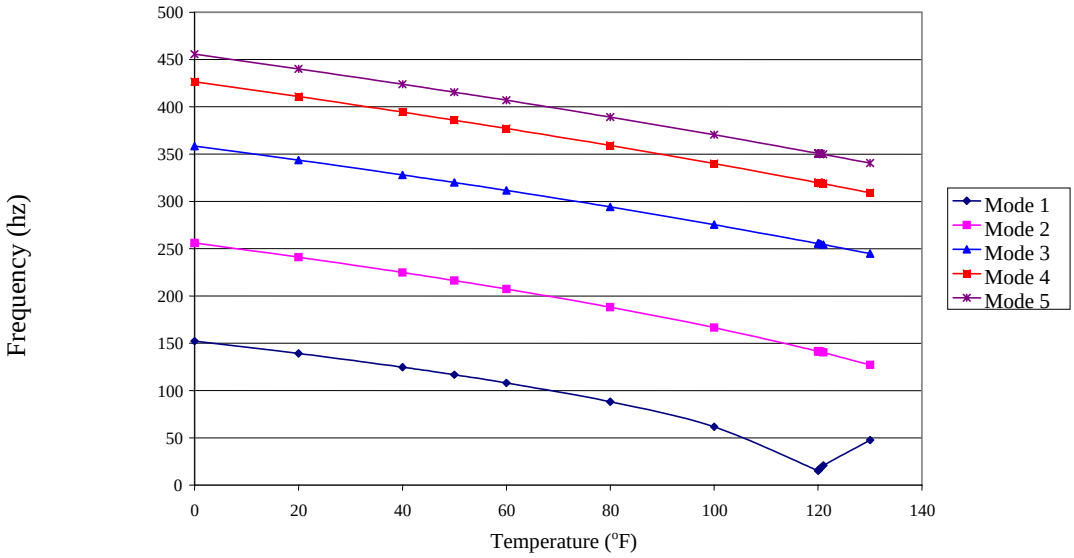

Figure 5.7 Graphs between the temperatures and frequencies for a 40 in x 30 in x 0.5 in plate for clamped boundary conditions showing the first 5 modes

The frequencies of the first five modes for the plate geometry 40 in x 30 in x 0.5 in for the simply-supported boundary conditions are shown in *Table 5.5*.

Table 5.5 Frequencies for a 40 in x 30 in x 0.5 in plate for simply-supported boundary conditions

Temperature (^{o}F)	Mode#1	Mode#2	Mode#3	Mode#4	Mode#5
0	81.7336	170.243	238.779	317.844	327.956
20	59.5926	150.006	218.924	298.412	308.408
40	20.547	126.574	197.079	277.623	287.535
41	16.301	125.288	195.923	276.542	286.451
42	10.4531	123.988	194.76	275.458	285.364
43	6.86932	122.674	193.59	274.369	284.272
43.015625	7.04473	122.654	193.571	274.352	284.255
43.03125	7.21697	122.633	193.553	274.334	284.238
43.0625	7.54758	122.592	193.516	274.3	284.203
43.125	8.16973	122.509	193.443	274.232	284.135
43.25	9.28985	122.344	193.296	274.096	283.998
43.5	11.1989	122.012	193.002	273.822	283.724
44	14.2703	121.346	192.413	273.275	283.176
50	52.0281	97.6744	172.489	255.146	265.023

Using the results from *Table 5.5*, graphs are plotted between the applied temperatures and obtained frequencies for the first five modes as shown in *Figure 5.8.*

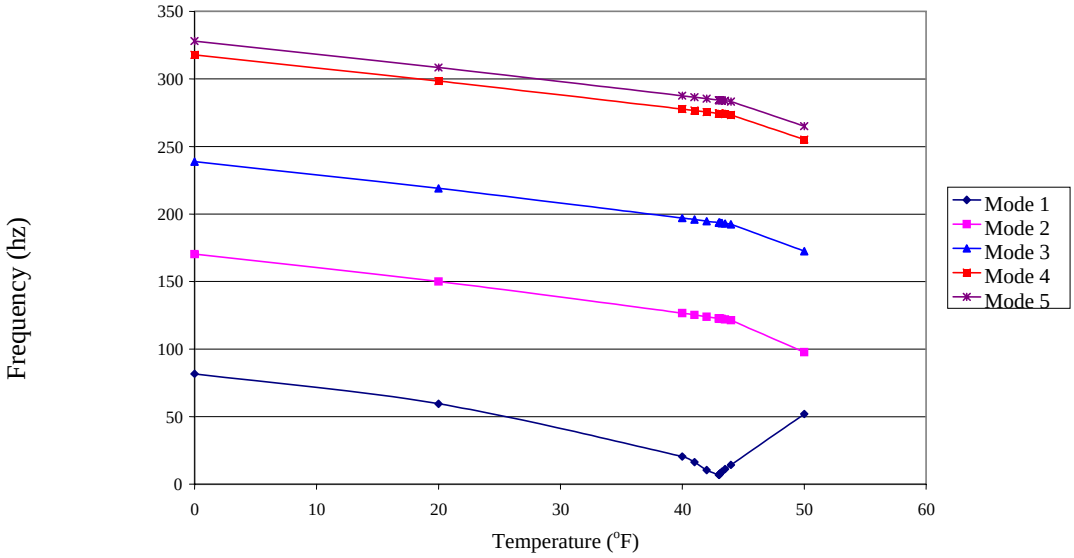

Figure 5.8 Graphs between temperatures and frequencies for a 40 in x 30 in x 0.5 in plate for simply-supported boundary conditions showing the first 5 modes

The frequencies for the plate geometry 40 in x 20 in x 0.5 in for the clamped boundary conditions are given in *Table 5.6*.

Table 5.6 Frequencies for a 40 in x 20 in x 0.5 in plate for clamped boundary conditions

Temperature (°F)	Mode#1	Mode#2	Mode#3	Mode#4	Mode#5
0	293.473	381.595	538.767	763.715	763.829
20	281.543	367.589	523.494	747.922	749.351

40	269.031	352.982	507.735	731.775	734.567
60	255.846	337.692	491.444	715.25	719.456
80	241.874	321.619	474.565	698.321	703.999
100	226.965	304.634	457.032	680.958	688.171
120	210.912	286.572	438.766	663.126	671.944
140	193.423	267.209	419.673	644.788	655.29
160	174.054	246.232	399.633	625.898	638.172
180	152.07	223.18	378.499	606.407	620.553
200	126.09	197.314	356.077	586.255	602.387
220	92.7736	167.325	332.112	565.372	583.623
250	49.7534	107.11	292.453	532.494	554.218
250.25	50.6812	106.462	292.1	532.212	553.966
250.5	51.5925	105.81	291.746	531.929	553.714
251	53.3689	104.494	291.038	531.363	553.21
252	56.7567	101.81	289.615	530.229	552.199
260	76.9981	78.8355	277.972	521.069	544.045
300	128.247	146.538	210.378	472.603	501.181

Using the results from *Table 5.6*, graphs are plotted between the applied temperatures and obtained frequencies for the first five modes as shown in *Figure 5.9.*

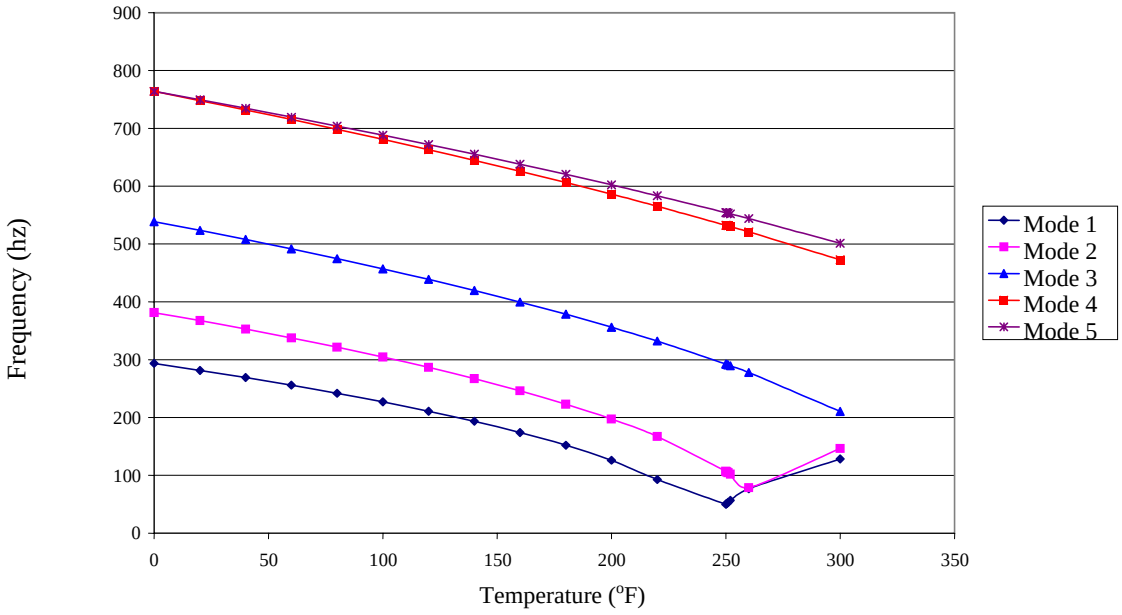

Figure 5.9 Graphs between temperatures and frequencies for a 40 in x 20 in x 0.5 in plate for clamped boundary conditions showing the first 5 modes

The frequencies for the plate geometry 40 in x 20 in x 0.5 in for the simply-supported boundary conditions are given in *Table 5.7*.

Table 5.7 Frequencies for a 40 in x 20 in x 0.5 in plate for simply-supported boundary conditions

Temperature (°F)	Mode#1	Mode#2	Mode#3	Mode#4	Mode#5
0	147.147	236.085	384.75	500.363	590.421
20	126.569	216.223	365.451	480.962	571.144
40	101.919	194.34	345.073	460.744	551.194

60	68.9569	169.659	323.415	439.597	530.494
80	29.6199	140.712	300.198	417.381	508.953
80.25	30.7854	140.313	299.896	417.096	508.678
80.5	31.9084	139.912	299.594	416.81	508.403
81	34.0434	139.107	298.99	416.239	507.852
85	47.8062	132.491	294.107	411.639	503.424
90	60.7744	123.725	287.888	405.817	497.833
100	80.6829	104	275.028	393.913	486.459

Using the results from *Table 5.7,* graphs are plotted between the applied temperatures and obtained frequencies for the first five modes as shown in *Figure 5.10.*

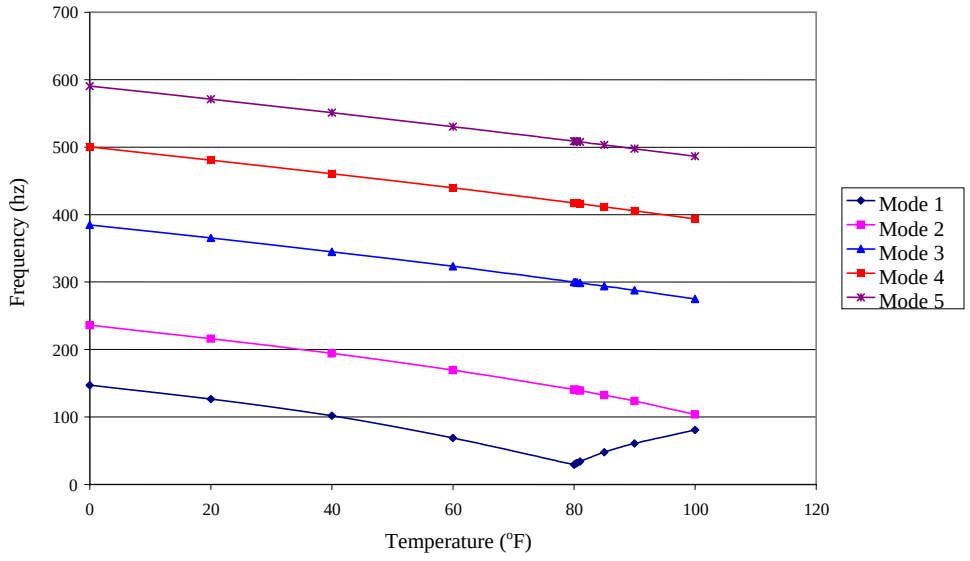

Figure 5.10 Graphs between temperatures and frequencies for a 40 in x 20 in x 0.5 in plate for simply-supported boundary conditions

5.2.3 Buckling under Localized Loads - Local Temperature Load

5.2.3.1 Analysis Procedures

1. Go to the ‘Start menu’ and pull up ‘Programs’, ‘Algor’, ‘Superdraw III’.
2. Go to ‘Add’, ‘Rectangle’ and construct a rectangle of length 40 in and breadth 30 in.
3. Go to ‘FEA Mesh’, ‘Automatic mesh’: ‘4 Point’ and then click on ‘Division values’ and enter the divisions as 20 and 20 in the AB and BC divisions boxes respectively.
4. Then, starting from one of the corners of the rectangle, right click on each of the four corners of the rectangle, in a clock-wise or anti-clockwise manner. By this, we are meshing it.
5. Transfer the model to the ‘FEA Editor’ by going to ‘File’, ‘Export to Fempro’.
6. A ‘Units definition’ screen appears. Click ‘OK’ to set it to the default units.
7. Set the ‘Analysis type’ to ‘Natural Frequency (Modal) with Load Stiffening’.
8. Set the ‘Element type’ to ‘Plate’.
9. Double click on the ‘Element definition’, and enter the thickness of the plate as 0.5 in and in the box named as ‘Temperature method’, change the option to ‘Nodal dT’, as we will use temperatures in this particular analysis.
10. Click ‘OK’.
11. Set the ‘Material type’ to ‘Steel (ASTM-A36)’.
12. Using the ‘Rectangular-select’ option, select the vertices of every side of the plate and clamp all the four sides of the plate for the clamped boundary conditions and similarly, constrain the necessary translations and rotations of the sides of the plate

for the simply-supported boundary conditions.

13. Now, select the entire plate using the ‘Rectangular-select’, and then apply the required temperature to it.
14. Next, select a small center patch within the plate and apply a temperature higher to it than the rest of the plate as shown in *Figure 5.11*.
15. Double click on the ‘Analysis parameters’ and enter a value of 1 in the ‘Thermal multiplier’ box, since we are taking temperatures into account.
16. Now, after setting up the model, along with the required boundary conditions and temperatures, click on the ‘Check model’ icon at the top toolbars; this is to run a check to see if everything was done right or not.
17. After checking the model, run the analysis.
18. After the analysis is done, the results of the analysis are displayed in ‘Superview’.
19. Record the first five natural frequency values that are displayed in the ‘Superview'.

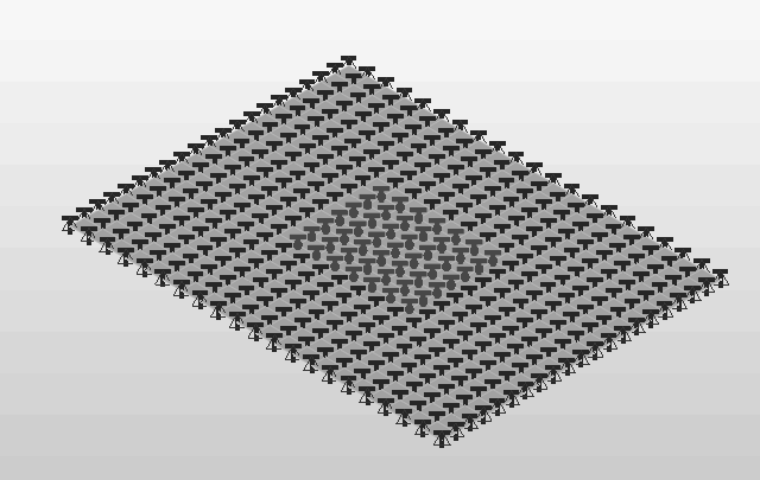

Fig 5.11 Plate Element showing the nodal temperatures

5.2.3.2 Analysis Results

The plate frequencies of the first five modes for the clamped boundary conditions are given in *Table 5.8*.

Table 5.8 Frequencies obtained for local temperature load for clamped boundary conditions

Temperature of the entire plate (^{o}F)	Temperature of a center patch within the plate (^{o}F)	Mode 1	Mode 2	Mode 3	Mode 4	Mode 5
0	50	144.309	248.602	350.475	418.463	451.431
0	100	135.549	240.758	342.152	409.946	447.084
0	150	125.85	232.505	333.484	401.103	442.655
0	200	114.92	223.782	324.437	391.908	438.141
0	250	102.294	214.515	314.972	382.333	433.537
0	300	87.1372	204.608	305.042	372.351	428.838
20	70	130.301	232.976	335.186	402.313	435.609

The plate frequencies of the first five modes for the simply-supported boundary conditions are given in *Table 5.9*.

Table 5.9 Frequencies obtained for local temperature load for simply-supported boundary conditions

Temperature of the entire plate (^{o}F)	Temperature of a center patch within the plate (^{o}F)	Mode 1	Mode 2	Mode 3	Mode 4	Mode 5
0	50	71.7646	162.327	229.882	309.144	323.513
0	100	59.9143	153.931	220.517	299.988	318.994

0	150	44.6409	144.962	210.615	290.309	314.394
0	200	18.7409	135.293	200.091	280.031	309.71
0	250	36.6871	124.746	188.836	269.062	304.938
0	300	55.7985	113.054	176.703	257.293	300.071
20	70	44.9409	140.956	209.182	289.125	303.679

Chapter 6

CONCLUSIONS

The ‘Natural frequency with load stiffening analysis’ used to calculate the effect of the in-plane loads on the natural frequencies of the beams and plates agreed with the ‘Critical buckling load analysis’.

In the ‘Critical buckling load analysis’, the computer may give a wrong load by missing the lowest one. This is indicated by a warning message which must not be ignored. To avoid any miscalculations by the algor program, the number of iterations must be increased gradually whenever the warning sign shows up to make sure that the solution has converged accurately within the given convergence limit specifications.

As the in-plane stress increases, the modal frequencies decrease. At the critical buckling load, the lowest mode has zero frequency. The load versus the square of the frequency follows a linear path.

REFERENCES

[1] Julian W. Gardner, V. K. Varadan, Osama O. Awadelkarim. *Microsensors, MEMS and Smart Devices*, Hardcover Edition. John Wiley & Sons, 2001.

[2] Henry Helvajian. *Microengineering Aerospace Systems*, AIAA, 1999.

[3] Gregory T. A. Kovacs. *Micromachined Transducers Sourcebook*. McGraw-Hill Inc., 1998.

[4] Eastman Kodak Company Web Site, 2004. http://www.kodak.com/country/US/en/corp/researchDevelopment/technologyFeatures/mems.shtml.

[5] MEMS and Nanotechnology Clearinghouse Web Site, Virginia, 2005. http://www.memsnet.org/

[6] Cambridge University, Engineering Department Web Site, Cambridge, UK, 2005. http://www.eng.cam.ac.uk/

[7] Tai-Ran Hsu. *MEMS &MICROSYSTEMS : Design and Manufacture*, 1st Edition. Mechanical Engineering Series, Mc-Graw-Hill International Edition, 2002.

[8] Wilhem T. S. Huck, Ned Bowden, Patrick Onck, Thomas Pardoen, John W. Hutchinson, and George M. Whitesides. : "*Ordering of Spontaneously Formed Buckles on Planar Surfaces*." Langmuir, 16: 3497-3501, 2000.

[9] Ned Bowden, Scott Brittain, Anthony G. Evans, John W. Hutchinson, and George M. Whitesides. : "*Spontaneous formation of ordered structures in thin films of metals supported on an elastomeric polymer.*" Nature, 393: 146-149, 1998.

[10] Department of Engineering Mechanics, University of Nebraska, Lincoln Web Site, 2000. http://em-ntserver.unl.edu/NEGAHBAN/Em325/21-buckling%20of%20columns/Buckling%20of%20columns.htm.

[11] ALGOR Web Site, 2005. http://www.algor.com/products/analysis_types/linear_dynamics/buckling.asp?sQuery=critical%20buckling%20load%20analysis.

[12] J. N. Reddy. *An Introduction to the Finite Element Method*, 2nd Edition. Engineering Mechanics Series, McGraw-Hill International Editions, 1993.

[13] Daniel J. Inman. *Engineering Vibration*, 2nd Edition. Prentice-Hall Inc., 2001.

[14] Yongsik Lee. *A Study of Beam Vibration with a Dry Frictional Joint*. University of Missouri-Columbia, M. S. Thesis, 2001.

[15] Robert D. Cook, David S. Malkus, Michael E. Plesha, Robert J. Witt. *Concepts and applications of Finite Element Analysis*, 4th Edition. John Wiley & Sons, Inc., 2002.

[16] Thomas J. Urbanik. : "*Review of Buckling Mode and Geometry Effects on Postbuckling Strength of Corrugated Containers*." ASME, 343: 85-96, 1996.

[17] B. Cotterell and Z. Chen. : "*Buckling and cracking of thin films on compliant substrates under compression*." International Journal of Fracture, 104: 169-179, 2000.

[18] A. L. Volynskii, S. Bazhenov, O. V. Lebedeva, and N. F. Bakeev. "*Mechanical buckling instability of thin coatings deposited on soft polymer substrates*." Journal of Materials Science, 35: 547-554, 2000.

[19] Le-Chung Shiau and Shih-Yyao Kuo. "*Thermal Buckling of Composite Sandwich Plates*." Mechanics Based Design of Structures and Machines, 32: 57-72, 2004.

[20] S. M. Sze. *Semiconductor Sensors*. John Wiley & Sons Inc., 1994.

[21] Robert D. Cook. *Finite Element Modeling for Stress Analysis*. John Wiley & Sons Inc., 1995.